PI3Kα activity in PHGDH-low pancreatic epithelial cells limits tissue proliferative regeneration in cancer promoting conditions

Cayron C[1,2], Bozoglou D[1,2], Villard A V[1,2], Reyes-Castellanos G[3], Therville N[1,2], Baer R[1,2], Arcucci S[1,2], Naud N[4], Tosolini M[1], Pont F[1], Ferreira Da Mota D[1,5], Guéraud F[4], Basset C[1,2,5], Carrier A[3], Pierre F[4], Thibault B[1,2], Dufresne M[1,2], Guillermet-Guibert J[1,2].

[1]INSERM, CNRS, Université Paul Sabatier, CRCT, Toulouse, France;
[2]Laboratoire d'Excellence TouCAN,
[3]Aix Marseille Univ, CNRS, INSERM, Institut Paoli-Calmettes, CRCM, Marseille, France
[4]Inrae, Toxalim, Toulouse, France
[5]Service d'Anatomo-Pathologie, IUCT-O, Toulouse

Short running head - PI3Kalpha and PDAC interception

Corresponding author: Julie Guillermet-Guibert
CRCT UMR1037 INSERM-Université Toulouse 3 - ERL5294 CNRS; 2 avenue Hubert Curien; Oncopole de Toulouse; CS 53717; 31037 TOULOUSE CEDEX 1 - FRANCE
Phone: +33-(0) 5 82 74 16 52
e-mail: julie.guillermet@inserm.fr
http://www.crct-inserm.fr/17-j-guillermet-guibert-sigdyn-group-pi3k-isoforms-signalling-cancerogenesis-559.html
http://eupancreas.com/julie-guillermet-guibert

Declarations of conflicts of interests

F Pierre, F Guéraud have some research projects from their academic research teams that have been co-financed by the processed meat sector. The other authors declare no conflict of interest.

Key words:
Pancreatic cancer, tissue renewal, inflammation, red meat consumption, metabolic enzyme, PI3K cell signalling

Summary (40 words) now 40

Red meat-enriched food, a pancreatic cancer risk factor, acts as an inflammatory stress for the pancreas. Inflammation dampens beneficial exocrine cell proliferative turnover and stimulates PI3Kα-dependent precancer lesions. PI3Kα inhibitors represent a pancreatic cancer prevention drug in patient with pancreatitis.

Summary max 160 now 160

Pancreatic exocrine cell plasticity promotes cancer (PDAC). Tissue damage by inflammation (pancreatitis) is repaired by plasticity but also by a beneficial proliferative regeneration. To identify molecular drivers of proliferative turnover, we compared human samples of pancreatitis and PDAC, the latter a condition with increased plasticity. We identified PI3K activation gene signatures and, amongst those, *PHGDH,* encoding an enzyme responsible for serine synthesis, as differentially expressed. Caerulein or red meat-enriched diet promotes pancreatic plasticity, PI3K activation, but also increased PHGDH. Interestingly, *in vitro*, pharmacological or genetic PI3Kα inhibition had differential action on the level of the p27 quiescence marker depending on the level of PHGDH controlling mitochondrial activity. *In vivo*, genetic inactivation of PI3Kα in the pancreas led to a reduced exocrine cell plasticity but to an increase of acinar cell proliferative markers. As PI3Kα inhibitors were shown to block plasticity while maintaining pancreas mass, they may represent a preventive interception drug in patients with pancreatitis at risk of developing cancer.

Introduction

Pancreatic ductal adenocarcinoma (PDAC) is one of the top five causes of death by cancer and its incidence is on the rise, particularly in <65y population (Siegel et al., 2017; Bouvier et al., 2017a; b; Siegel et al., 2023). Inflammatory conditions are generally thought to set the soil for cancer initiation and to share common molecular induction pathways with neoplasia, explaining the increased prevalence of cancers in patients with chronic inflammation. For patients with hereditary pancreatitis or with chronic pancreatitis (CP) from all etiologies (alcoholic, hereditary, obstructive, autoimmune), pancreatic cancer represents a serious complication (Kleeff et al., 2016b, 2017; Kirkegård et al., 2018). Acute pancreatitis (AP) is one of the most frequent gastrointestinal causes of hospital admission; chronic pancreatitis is lower in incidence, but represents a very invalidating condition (Kleeff et al., 2017). The burden of all these pancreatic disorders is expected to increase over time. They also share with initiation of cancer common events of transformation of the parenchyma, such as the transdifferentiation of acinar exocrine cells into duct cells defining acinar-to-ductal metaplasia (ADM).

Pancreas is described as a plastic organ, where differentiated cells are facultative progenitors able to transdifferentiate in other differentiated cell types (Zhou and Melton, 2018; Kopp et al., 2012; Stanger and Hebrok, 2013; Storz and Crawford, 2020). The transdifferentiation of acinar cells (in charge of digestive enzyme production and their controlled secretion) in ductal cells (the other exocrine cells, lining the pancreatic duct, that product bicarbonate-rich secretion), called ADM, is occurring during the early onset of inflammation. Recently, it was demonstrated that this acinar-to-ductal plasticity promotes an epigenetic reprogramming, called epithelial memory of inflammation, which favours cancer initiation (Del Poggetto et al., 2021).

It is now well accepted that there are also other inflammatory conditions than CP and AP that predispose to pancreatic tumour development, such as diabetes (Klein, 2021; Puri et al., 2015; Molina-Montes et al., 2018; Shen et al., 2023; Kleeff et al., 2016a; Friedlander et al., 2009). Increased consumption of red and processed meat is an epidemiologically validated risk condition (Petrick et al., 2020; Nöthlings et al., 2005), but the underlying mechanisms and whether it is related to increased pancreatic inflammation or induction of ADM are unknown.

At the inception of these pathologic conditions, not all acinar cells transdifferentiate in response to stress. The exocrine lineage also responds to various stresses also through increased proliferation (Zhou and Melton, 2018). Unlike tissues that constantly renew themselves such as intestinal crypts, it is generally considered that no dedicated adult stem cells or stem cell niche are present in the pancreas to recover the tissue homeostasis and repair the damaged tissue. Instead, the proliferation of acinar cells that maintain their differentiation status helps to replace the damaged apoptotic acinar cells. Understanding early molecular events of exocrine pancreas plasticity/proliferation balance occurring during pancreatic inflammatory conditions is critical to predict and support the treatment of patients at higher risk of developing pancreatic cancer.

Phosphoinositide-3-kinases (PI3Ks) are major actors of cell homeostasis, producing signalling lipids at the plasma membrane. These lipids activate downstream effectors such as AKT (Vanhaesebroeck et al., 2010) by a cascade of phosphorylation events, leading to the regulation of protein synthesis, cell proliferation, survival, growth, migration, and metabolism, and actin remodelling, but also gene expression. Inhibition of all PI3Ks by wortmannin, of PI3Kα by A66, GDC-0326 or BYL-719 or of the immune-restricted PI3Kγ by genetics prevents the induction of acute pancreatitis both by preventing ADM and by reducing immune cell recruitment (Lupia et al., 2004; Baer et al., 2014; Thibault et al., 2021; Pandol et al., 2007; Gukovsky et al., 2004). Mutated KRAS, the most frequent initiating oncogenic mutation in PDAC, is found in 90% of pancreatic cancer patients, and the research of *KRAS* mutations within endoscopic ultrasound - fine needle aspiration/biopsies (EUS-FNAB) improves the diagnosis of PDAC in pancreatitis context (Bournet, 2014). PI3Kα is critical for ADM and for the induction of pancreatic cancer by oncogenic KRAS in the presence of mutated p53 and / or concomitant inflammation (Baer et al., 2014; Wu et al., 2014). Inflammation was shown to prevent oncogene-induced senescence and thus to be permissive for pancreatic cancer initiation (Guerra et al., 2007).

Because PI3Kα is so critical for the early induction of cell transformation at the origin of pancreatic cancer, we sought to determine the importance of the PI3K signalling pathway in pancreas subjected to repetitive stress, to search for a potential link between PI3K-driven ADM lesions in pancreatitis with pancreatic acinar cell proliferation. Because PI3K inhibitors blocked pancreatic plasticity but maintained pancreatic mass, we found that the clinically available PI3Kα inhibitors are compatible with their use as cancer prevention drugs in pancreatitis context.

Results

PI3K/AKT pathway gene signatures and *PHGDH* are differentially expressed in chronic pancreatitis compared to pancreatic adenocarcinoma

Context is known to influence the output of cell signalling pathways. We sought to determine in an unbiased manner which signalling pathways are selectively associated with risk condition for cancer development such as CP compared to primary tumour of PDAC.

We analysed publicly available datasets to distinguish chronic pancreatitis (CP) from primary tumours of PDAC (PDAC) (Fig. 1a-c, Suppl. Table 1). CP and PDAC patients presented differential enrichment of mRNA expression-based hallmarks of biological pathways, also enriched compared to normal, in 22 hallmarks. The PI3K/AKT/mTOR signalling pathway was found in the top five of the most differentially expressed with the lowest p-value (Fig. 1a). Differential enrichment analysis demonstrated that selective PI3K/AKT/mTOR pathway signatures were enriched in CP and in PDAC compared to normal parenchyma (Fig. 1b): this is what emerged from Reactome pathway analysis. In detail, we found that PI3K cascade to FGFR1-4 were significantly increased in CP as opposed to PDAC and normal parenchyma, suggesting differential activation of receptor tyrosine kinase (RTK)-coupled PI3K in these samples (Fig. 1b). Reversely, PI3K cascade to ERBB2, that have known role in PDAC initiation downstream KRAS (Ardito et al., 2012; Navas et al., 2012; Blasco et al., 2019; Meyers et al., 2020; Grimont et al., 2015), was significantly increased in PDAC as opposed to CP and normal parenchyma. Considering that PI3Kα is key for RTK signalling (Graupera et al., 2008) and PDAC initiation and progression (Baer et al., 2014; Thibault et al., 2021), we then used the previously published PI3Kα activation gene signature, based on expression levels of PI3Kα activation-associated curated genes (Thibault et al., 2021). PI3Kα activation scoring allowed us to cluster together all CP patients from two different aetiologies (Fig. 1c). Conversely, PDAC clustered mostly with activated stroma of CP. Amongst the list of genes in the signature, *PHGDH* stroke as enriched in the CP-rich cluster. PHGDH oxidizes the glycolytic intermediate 3-PG into 3-PHP (rate-limiting step in serine synthesis from 3-PG) and controls ROS detoxification in cancer settings (Li and Ye, 2020).

To confirm the relevance of these findings in animal models, we compared gene expression upon two sequential injections of caerulein (Kong et al., 2018), a stable form of cholecystokinin (CKK) that promotes pancreatic inflammation, in mice non harbouring (mimicking inflammatory condition, a condition at risk for developing cancer) or harbouring mutant KRASG12D (mimicking early steps of cancer) (Fig. 1d). Similarly, while PI3K/AKT activation signature was evolving in a similar manner in both groups of mice (Fig. 1e), the PI3K events in ERBB2 signalling or the PI3K events in FGFR2 signalling were significantly enriched in mutant KRAS (precancer) or in WT pancreas (inflammation only), respectively (Fig. 1f,g). The expression of *PHGDH* was enriched differently in time in WT in comparison to KRAS-oncogenic model (Fig. 1h).

Hence, PI3K/AKT activation signatures is associated with a differential PI3Kα activation signature in both chronic pancreatitis and PDAC. Amongst the genes which expression is associated with PI3Kα, *PHGDH* levels were increased in CP and inflammation only condition, suggesting a role in pancreatic regeneration.

Nutritive stress promotes bulk PHGDH increased levels and is associated with PI3K activation and a decrease of proliferative markers

The CCK analog caerulein stimulates the exocytosis of digestive enzymes by pancreatic acinar cells; its natural counterpart CCK is normally secreted when food is ingested. The amount of the

analog of CCK that we inject in mice is in excess and in a stable form; this leads to excessive secretion of digestive enzymes, loss of epithelial barrier and pancreatic inflammation (Fig. 2a,b). In this experimental model, we validated the bioinformatics data (Fig. 1c,h) by confirming that pancreas subjected to repetitive caerulein injection (Fig. 2a) presented an inflammation (Fig. 2b) and a significantly higher level of PHGDH (Fig. 2c). We next hypothesized that caerulein treatment could mimic a physiological situation when red meat-enriched diet would trigger an inflammation. We decided to compare pancreas from rats that had access to control diet or to a diet enriched in red meat, known to increase the risk of PDAC (Petrick et al., 2020). This later nutritive regimen is called from there Meat diet (Fig. 2d) and was associated selectively with the presence of ADM lesions in rat pancreas (Fig. 2e). Indeed, pancreatic ADM lesions indicative of increased acinar cell plasticity were observed only in the cohort of rats that had Meat diet (Fig. 2e). We analysed PHGDH level by Western blotting amongst the most differentially expressed molecular markers identified in Fig. 1. Meat diet increased the level of pS473AKT (Fig. 2f,g), indicative of PI3K activation, and also of αSMA, indicative of stromal cell activation by inflammation (Fig. 2f,g). Interestingly, PHGDH protein level was also increased (Fig. 2f,g). To analyse possible regeneration process by proliferation, the cyclin-dependent kinase (cdk) inhibitor p27 (Jeannot et al., 2015) level was assessed and, despite the increase of PI3K activation usually associated with decreased cdk inhibitor expression (Bousquet et al., 2006), p27 level was significantly increased (Fig. 2f,g).

Collectively, these data show that repetitive stress both promotes PI3K activation and PHGDH level increase; those molecular events are associated with increased cell plasticity and increased level of anti-proliferative markers. These data led us to the hypothesis that activation of PI3Kα and altered levels of PHGDH could determine the level of proliferative regeneration in exocrine cells in stress conditions.

PI3Kα promotes proliferation only of PHGDH-high acinar cells

Interestingly, PHGDH immunohistochemistry analysis showed increased levels of PHGDH induced by caerulein only in acinar cells and not in ADM structures in pancreas (Fig. 3a).

To test whether the proliferative capacity of plastic exocrine cells in stressed pancreas is controlled by PI3K activity, we setup an *in vitro* model, using rat acinar AR-42J cells treated with a cocktail of EGF and dexamethasone (Dex + EGF) every 2 days that mimics the biochemical cues found *in vivo* in stressed pancreas and that promotes their plasticity from acinar to duct-like cells (Al-Adsani et al., 2010). After 8 days of treatment, morphology changes were associated with loss of acinar cell markers (*CK7*, *PTF1A*, *CTRC*, *MIST1*) without increased expression of ductal marker (*CK19*) (Fig. 3b,c), indicative of an intermediate stage of metaplasia from now called ADM-like. Some mRNA levels of PI3Kα activation signature decreased (*PTTG1, KIF2C, CCNB1, BCL2, CEP55, RRM2, CDC20, CCNE1)* were decreased in ADM-like cells (Fig. 3d); these genes corresponded globally to the genes decreased in PC patients (Fig 1c), while increased levels of those mRNAs corresponded to enrichment in pathways promoting proliferation (e. g. cell cycle (GO:0007049); Fig. 3e). PHGDH level was decreased in ADM-like cells (Fig. 3f) as observed *in vivo* (Fig. 3a). Treatment with PI3Kα inhibitor GDC-0326 decreased the level of pSer473AKT in both cell context (Fig. 3g-h), suggesting that both cell states harbour a PI3Kα activity. However, the level of cdk inhibitor p27 was increased by GDC0326 treatment in acinar cells (Fig. 3g) but not in ADM-like cells (Fig. 3h). Thus, the antiproliferation action of PI3Kα inhibition is observed only in PHGDH-high acinar cells.

Genetically reduced levels of PHGDH by transfection of pools of siRNA targeting *PHGDH* in acinar cells mimicked DEX+EGF treatment and decreased p27 levels to levels found in ADM-like cells (Fig. 3i,j). Treatment with the pharmacological inhibitor of PHGDH (CBR-5884) in acinar cells that most efficiently inhibited PHGDH activity *in vitro* (Suppl. Fig. 1) prevented the effect of GDC-0326 inhibitor on p27 expression level (Fig. 3k).

Both PI3Kα and PHGDH control mitochondrial activity (Li and Ye, 2020; Goncalves et al., 2018; Arcucci et al., 2021). To understand the mechanism of this differential effects of PI3Kα inactivation in a PHGDH-dependent manner, we analysed mitochondrial activity with Seahorse technology in AR42J cells with high (acinar) and low (ADM-like) PHGDH levels and measured the

effects of GDC-0326 PI3Kα and CBR-5884 PHGDH inhibitors alone or in combination (Fig. 3l-o). In cells with high PHGDH level (acinar), the combined treatment using GDC-0326 and CBR-5884 reduced and homogenised the mitochondrial maximal capacity compared to these inhibitors alone (Fig. 3l,m), while the single combinative treatment had little or no effect in cells with low levels of PHGDH (Fig. 3n,o).

Finally, we studied primary *ex-vivo* cultures of acinar cells from murine pancreas, which are known to spontaneously transdifferentiate. We inactivated PI3Kα catalytic enzyme with a genetic approach designed to prevent compensations between isoforms of PI3Ks and to mimic pharmacological inactivation, by deleting the PI3K catalytic domain (Arcucci et al., 2021; Guillermet-Guibert et al., 2008) in adult acinar cells selectively (Grimont et al., 2015). Using ElastaseCreER+;p110αflox/flox mice (α^{in}E), we genetically inactivated PI3Kα in acinar cells promoting the recombination of two exons encoding p110α catalytic domain by CreER expression in Elastase-positive cells (acinar cells) and by tamoxifen treatment *in vivo*; control Cre negative mice (CT) were also tamoxifen treated. Exocrine cell preparation was performed, cultured *ex-vivo* to promote spontaneous transdifferentiation, and EdU incorporation was analysed to monitor DNA replication/proliferation (Fig. 3p,q). As expected, the proliferation rate of ElastaseCreER-positive tamoxifen-treated pancreatic exocrine cells was unchanged compared to the ElastaseCreER-negative tamoxifen-treated pancreatic exocrine cells(Fig. 3m).

The inactivation of PI3Kα increases p27 in PHGDH-high acinar cells; the antiproliferation action of PI3Kα inhibition is observed only in PHGDH-high acinar cells.

***In vivo* genetic or pharmacological down-regulation of PI3Kα activity increases the number of proliferating acinar cells after stress**

Finally, we aimed to test *in vivo* whether by blocking plasticity in PHGDH-low cells but not preventing their proliferation, PI3Kα catalytic inactivation could be beneficial to promote acinar cell proliferation and pancreas regeneration. If so, clinically used therapeutic agents against PI3Kα could be used as a prevention strategy against development of precancer ADM lesions while maintaining the proliferative potential of exocrine cells.

Knowing that repetitive stress was sufficient to increase PHGDH level in acinar cells and to decrease its level in ADM (Fig. 2b, Fig. 3a), we tested whether the sole genetic catalytic inactivation of PI3Kα altered the proliferation rate of acinar cells *in vivo*. We deleted the exons encoding PI3Kα catalytic domain selectively in pancreatic epithelial lineage (α^{in}C model). Cre recombinase expression in Pdx1-positive cells induced the deletion of two exons encoding the catalytic domain of PI3Kα (Suppl. Fig. 2a). We subjected WT or α^{in}C mice to eight series of caerulein injections over 17 days to induce a repetitive stress (Fig. 4a). Pancreatic cell-specific genetic inactivation of PI3Kα did not prevent caerulein-induced hypersecretion of acinar cells as measured by similar levels of plasmatic amylase at early time points (Suppl. Fig. 2b). PI3Kα inactivation led to decreased levels of pAKT substrate staining (Suppl. Fig. 2c), blocked the onset of pancreatic injury, quantified by a significantly decreased pancreatitis score (Fig. 4b), fibrosis (Suppl. Fig. 2d,e) and the number of ADM lesions (with quantified Metaplasic ducts, Fig. 4c). ADM occurs upon re-expression of key pancreatic progenitor factors (Kopp et al., 2012). We confirmed that nuclear Sox9 re-expression by caerulein was significantly decreased by genetic PI3Kα inactivation (Fig. 4e; Suppl. Fig. 2f).

Next, we analysed the caerulein effects on cells with acinar morphology. Caerulein-induced acinar cell atrophy was blocked by PI3Kα inactivation (Fig. 4d), a moderate loss of amylase expression was observed in PI3Kα–deficient cells that maintained an acinar morphology compared to vehicle WT condition (Fig. 4d). The duct-specific marker cytokeratin 19 (CK19) was expressed in an increased number of duct-like structures in caerulein-treated WT cells but presented a moderate basolateral expression in cells with acinar morphology when PI3Kα was inactivated (Fig. 4d). This was associated with an increase of the proliferation Ki67 marker in caerulein-treated PI3Kα–deficient acinar cells compared to caerulein-treated WT acinar cells (Fig. 4f). We confirmed the action of PI3Kα inactivation on controlling cell cycling by examining quiescence marker p27: p27 nuclear expression was further significantly decreased by PI3Kα inactivation in caerulein-treated acinar cells (Fig. 4g +

Suppl. Fig. 2f). Under the stress promoted by repetitive injection of caerulein, PI3Kα catalytic inactivation largely maintained a proliferative regenerative response in the pancreatic exocrine parenchyma, which kept their acinar morphology.

To confirm the relevance of these findings for translational application, we next verified whether a pharmacological inactivation of PI3Kα would mimic the genetic inactivation of PI3Kα in pancreatic lineage. *In vivo*, a pharmacological inhibition of PI3Kα by GDC-0326 prevented the damage of repetitive injection of caerulein, while we only observed some isolated ADM and in lower numbers (Fig. 4h,i). Interestingly, GDC-0326 treatment led to the absence of fibrosis accumulation (Fig. 4i, picrosirius staining), suggesting that PI3Kα activity in stromal cells might also contribute to pancreatitis-induced lesions.

PI3Kα activity promotes acinar cell plasticity, known to increase the risk to develop cancer. Reversely, PI3Kα genetic or pharmacological inactivation changes acinar cell fate under stress and promotes proliferative acinar cells that could also sustain pancreatic regeneration.

Discussion

Determining the precise molecular links between chronic inflammatory disease, epidemiologically identified risk factor conditions and PDAC is necessary to predict which patients are at higher risk of developing this lethal disease. Here, we demonstrate that, in epithelial cells, the signalling enzyme PI3Kα positively contributes to a detrimental fate of acinar cells in repetitively injured pancreas by caerulein or by red meat-enriched diet. PI3Kα activity both promotes acinar cell plasticity and prevents regeneration by cell proliferation (Fig. 4j, **Graphical abstract**). Mechanistically, PI3Kα activity and PHGDH levels cooperate in stressed acinar cells to control the cdk inhibitor p27 level and the fine tuning of mitochondrial activity, necessary to those processes.

Both PI3K and MAPK pathways are activated during pancreatic injury. PI3Kα controls actin-cytoskeleton remodelling necessary for ADM (Baer et al., 2014); while pancreas-restricted inhibition of MAPK pathway via short hairpins targeting MEK1/2 or their systemic inhibition via a pharmacological inhibitor trametinib (generic name) prevents the formation of ADM <u>and</u> the turnover of pancreatic parenchyma (Halbrook et al., 2017). It is interesting to note from our data that PI3Kα inhibition increases the turnover of pancreatic cells. Hence, the inhibition of PI3Kα signalling could potentially prevent the formation of precursor lesions in the pancreas while maintaining the regenerative capacities of the pancreas.

Strobel et al. suggested early on that the absence of expression of the HPAP reporter in exocrine lineage after pancreatic injury was indicative that acinar-to-ductal or acinar-to-centro-acinar transdifferentiation could occur, but that this process did not contribute significantly to exocrine regeneration (Strobel et al., 2007). Stem/progenitor cells only represent a small proportion of the pancreas (Wollny et al., 2016). However, pancreatic injury leads to transient re-expression of progenitor factors in all acinar cells (Kopp et al., 2012; Jeannot et al., 2015), that is prevented in our study by PI3Kα inactivation. ADM participates in the intrinsic defence mechanism towards pancreatic injury by reducing intra-tissular or systemic leakage of activated digestive enzymes.

The pancreas does not have a high basal rate of cell proliferation compared to other digestive epithelia such as colon or intestine. Recent single-cell analysis uncovered that this increase of proliferating acinar cells comes from heterogenous exocrine cell subsets during pancreatic regeneration (Wollny et al., 2016). PI3Kα genetic and pharmacological inactivation was previously demonstrated by us and others to prevent oncogenic transformation (Baer et al., 2014; Wu et al., 2014). We demonstrate here that PI3K inactivation induces an increase of the pool of proliferating cells, while Kong et al showed that proliferating acinar cells are refractory to oncogenic Kras-transformation (Kong et al., 2018). Understanding this balance is critical to prevent cancer formation in an inflammatory context.

The metabolic enzyme PHGDH is overexpressed in triple-negative breast cancers (TNBC) and some other cancers such as melanoma (Locasale et al., 2011; Possemato et al., 2011). There is an extensive body of literature showing that increased PHGDH catalytic activity is important for (cancer cell) proliferation (Ma et al., 2021; Pacold et al., 2016; Ngo et al., 2020). Accordingly, average high

PHGDH gene expression has been associated with poor prognosis in multiple tumor types (Zhao et al., 2020). Our findings add a new level of understanding to the biology of PHGDH by showing that low level PHGDH protein expression is associated with cells undergoing pancreatic plasticity and that PI3Kα activity in those cells promoted their transdifferentiation. Their plasticity capacity is also associated with a sustained mitochondrial activity. This finding does not contradict previous data but echoes with the recent findings on metastatic breast cancer (Rossi et al., 2022): PHGDH-low cancer cells in the primary tumour are in a slow cycling state, but have increased metastatic behaviour, usually linked to plastic properties such as epithelial-to-mesenchymal transdifferentiation potential. Overall, we highlight the importance of differential regulation of PHGDH protein level in cell plasticity. Mechanistically, PHGDH critically reroutes glycolytic flux in stress situation; as such, its activity is an important mechanism of ROS detoxification (Riscal et al., 2016). Interestingly, imbalances of plasma amino acids and pain in chronic pancreatitis (CP) patients were measured and a glutamine supplementation was empirically associated with decreased pain (Kawaguchi et al., 2015). Based on work showing that PHGDH inhibition induces broad changes in cell metabolism (Reid et al., 2018), we could speculate that red meat-enriched food that promote alteration of PHGDH levels could disturb amino-acid and nucleotide homeostasis in pancreas.

Cancer interception is the active way of combating cancer and carcinogenesis at earlier stages. Acinar cells, albeit to a lesser extent than ductal cells (Bailey et al., 2016), are intrinsically refractory to cancerogenesis; expression of oncogenic KRAS is required for cell transformation, but is not sufficient to drive cancerogenesis (Carrière et al., 2011; Guerra et al., 2007). Small molecule inhibitors of all PI3K and selective of PI3Kα are currently in various phases of clinical trials (Pons-Tostivint et al., 2017) and could be used to prevent cell plasticity while maintaining regenerative potential of pancreas. We hope that, with the rapidly developing techniques allowing detection of circulating premalignant cells and fragmented DNA (Bournet, 2014) that allow to detect early disease also in preclinical models (Thibault et al., 2021), we will be able to propose strategies to prevent pancreatic cancer in population at risk. Pharmacological inhibition of pro-cancer pathways such as those driven by PI3Kα could then be tested as a preventive strategy in patients at risk for pancreatic cancer development.

Material & Methods

Transcriptomics data retrieval and bioinformatic analysis

PI3Kα gene signature was designed as the intersection of genes up- and down-regulated by shRNA against PIK3CA in a human PIK3CA mutated breast cancer cell line (Bosch et al., 2015) and PI3ka_human_LINCS_CMAP and PI3Ka_human_mTOR_CMAP LINCS gene signatures (Zhang et al., 2017), as described in (Thibault et al., 2021). Amongst the publicly available micro-array repositories, we selected transcriptional profiling datasets of normal pancreas, chronic pancreatitis and pancreatic cancer tissues, including 8 normal, 9 pancreatitis (alcoholic or autoimmune), 5 stroma of chronic pancreatitis (undocumented aetiology) and 7 pancreatic adenocarcinomas. Published data on human samples were retrieved from public databases (E6MEXP-804(Löhr et al., 2010), E-MEXP-1121(Rückert et al., 2008), E-TABM-145 (Vaquerizas et al., 2009)) from compatible platforms, normalized using RMA method (R 3.2.3, bioconductor version 3.2), collapsed (collapse microarray), filtered (SD>0.25), and statistically tested using an ANOVA test corrected with Benjamini & Hochberg method (BH). Published murine mRNA expression during experimental pancreatitis (GSE65146) was analysed by TTCA package of R (kindly corrected by its conceptor) and normalised with SCAN(Albrecht et al., 2017). For each sample, individual scoring for hallmarks or Reactome (actualised list of genes downloaded from MSigDB version [software.broadinstitute. org/gsea/msigdb] and Reactome [www.reactome.org]) was performed using Autocompare_SES software (available at https://sites.google.com/site/fredsoftwares/products/autocompare_ses) using the "greater" (indicating an enriched gene set) Wilcoxon tests with frequency-corrected null hypotheses (Tosolini et al., 2016), followed by values in each compared group using an ANOVA test. Hierarchical sample clustering was performed using the PI3Kα activation signature.

Reagents

Reagents were purchased as follows: BYL-719 (MedChem Express), CBR-5884 (MedChem Express), NCT-503 (MedChem Express), Caerulein from Bachem (ref. 4030451), Dexamethasone (Sigma-Aldrich, D1756), EGF (R&D Systems, 236-EG-200), Tamoxifen (MedChem Express). GDC-0326 was a gift from Genentech (*in vitro* IC50 in nM: p110α: 0.2; β: 133; δ: 20; γ: 51; C2β: 261; C2α>10µM; vps34: 2840; K_i mTOR in nM: 4300)(Heffron et al., 2016).
For in vitro experiments, GDC-0326 powder is resuspended at 10mM in DMSO then diluted as indicated. BYL-719 power is resuspended at 10mM in DMSO then diluted as indicated. CBR-5884 and NCT-503 powders are resuspended at 10mM in DMSO, sonicated at 4°C for 10min (10 cycles 30sec sonication + 30 sec stop) then diluted in medium as indicated.
For in vivo experiments, the powder is dissolved in 0.5% methylcellulose containing 0.1% Tween 80 (Sigma) using vortex and rotate at 4°C for 15 minutes. The solution is then sonicated at 4°C for 10min (10 cycles 30sec sonication + 30 sec stop). Solution is transferred into a wheaton vial. The solution is mixed well before administration. Dosing volume is 4mL/kg for PO dosing.

Genetically engineered mouse models
The LSL-Kras^{G12D} (from D Tuveson, Mouse Models of Human Cancers Consortium repository (NCI-Frederick, USA), Pdx1-cre (from DA Melton, Harvard University, Cambridge, MA, USA)(Gu et al., 2003), p110α^{lox} (from B. Vanhaesebroeck, UCL, London), Elastase CreERT2 mice (Elas-CreERT2) were generated by DA Stoffers (Philadelphia, PA, USA) and were kindly provided by Pr P Jacquemin (UCL, Belgium). Strains were interbred on mixed background (CD1/C57Bl6) to obtain compound mutant Pdx1-Cre;LSL-Kras^{G12D} (named KC), pdx1-Cre;p110α$^{lox/lox}$ (Pdx1-Cre;p110α$^{lox/lox}$ were named α^{in}C; pdx1-Cre;LSL- Kras^{G12D};p110α$^{lox/lox}$ were named Kα^{in}C) or Elas-CreERT2; p110α$^{WT/WT}$ (CT mice), Elas-CreERT2; p110α$^{lox/lox}$ (α^{in}E mice). For experiment with Pdx1-Cre, littermates not expressing Cre as well as Pdx1-Cre and p110α$^{lox/lox}$ mice of the same age were used as control; for experiments with Elastase CREERT2, CT mice injected with tamoxifen are controls. Seven week-old α^{in}E and CT mice were treated with tamoxifen (Sigma-Aldrich) dissolved in corn oil containing 10% ethanol at a concentration of 20 mg/ml. Mice received one intra-peritoneal (i.p.) injections (1 mg/15 g of body weight) on three consecutive days (Diakopoulos et al., 2015). All procedures and animal housing are conformed to the regulatory standards and were approved by the Ethical committee according to European legislation translated to French Law as Décret 2013-118 1st of February 2013 (APAFIS 3601-2015121622062840; APAFIS#32411-2021070616504074). Genotyping was performed as described in (Baer et al., 2014; Thibault et al., 2021): the genetically modified allele is called p110α^{lox} or p110α$^{\Delta DFG}$ (here named Rec) after Cre recombination. DFG is a conserved motif in the activation loop of the p110α kinase domain critical for its catalytic activity. The gene targeting strategy used is different from a traditional conditional knock-out strategy. Instead, it is deleting two exons in the catalytic domain of *Pik3ca* in the 3' part of the gene, allowing expression of a truncated inactive p110α after recombination. Primers corresponds to post-cre primers used to verify the presence of recombined allele ΔDFG: ma9: ACACACTGCATCAATGGC; ma5: GCTGCCGAATTGCTAGGTAAGC; annealing temperature: 65°C; recombined ΔDFG: 544 bp, wild type (+) or unrecombined lox: >10kbp amplicon. Genotyping of tail or pancreas samples was performed after DNA extraction with Sigma kit (XNAT-100RXN). Genotyping primers for Elastase CreERT2 are: ElasCreERT2 ElasF-CTCTGCTAACCATGTTCATGCCT ElasR-ACGCTAGAGCCTGTTTTG.

Repetitive caerulein-induced pancreatic injury & PI3K inhibitor in vivo dosage
Pancreatic injury was induced on young mice (8-12 weeks) by series of six hourly intra-peritoneal injections of caerulein (75µg/kg of body weight) that was repeated every 2 days in the presence or absence of GDC-0326 (10mg/kg). Animals were euthanized at 7 days, and recombination was verified before analysis as described in (Graupera et al., 2008; Guillermet-Guibert et al., 2008). GDC-0326 (10mg/kg) was administrated by gavage every morning. Amylase measurement was performed using

Phadebas kit (Phadebas Magle, used as suggested) in plasma samples at early time points. As a read-out of efficient pancreatic PI3Kα inhibition, glycemia was determined from tail blood using a glucose monitor (Accu-Chek Performa).

Histology and Immunostaining

Immunostainings were conducted using standard methods on formalin-fixed, paraffin-embedded tissues, including both mice and human pancreas. Antigen retrieval and antibody dilution was carried out as described in Supplementary Table 2. Picrosirius Red was from from Sigma, Direct Red 80 (used as suggested and analysed under polarized light.

Specific following settings were used for quantification of Ki67 (5 slides at 10x / mouse; Image J: Threshold Color, 8bit, Threshold, Watershed, Compting particles (0-infinity for pixel number, circularity: 0.1-1). The other qualifications were done manually in a blind fashion with slides ranged per intensity prior starting of the quantification.

Rats

Five-week-old male Fischer 344 rats were purchased from Charles River (France). Animal experiment was authorized by the French Ministry for Higher Education, Research and Innovation (MESRI) in accordance with the local ethic committee evaluation (APAFiS #16139-2018071617502938v3). Rats were randomly assigned to their respective groups and cages randomly placed in the animal facility. They were allowed to one-week acclimatization with Control diet before being i.p. injected with azoxymethane (Sigma-Aldrich) (20mg/kg) in buffered saline solution, in order to initiate colorectal cancer, as those rats were also used for a colorectal cancer study (Raju, 2008). Experimental diets started one week after azoxymethane injection, for 100 days. Rats had unlimited access to tap water and diet, given every day just before rat active period to limit food oxidation. All diets were based on modified low calcium AIN-76 diets with two powder composition: one for rat acclimatization and Control diet group with 32% protein as casein, and one, with no protein, to complement meat in the Meat diet group. These powders were prepared by SAAJ (INRAE, Jouy-en-Josas, France). All diets contained 5% safflower oil (MP Biomedicals 102888). Meat diet included pieces of cooked red meat (87,6 % of meat) and ham (12.4 % of meat) (beef sirloin was purchased from Picard, France and cooked ham from "Votrecharcutier.fr", France). Both diets were balanced for protein and lipid contents (the control diet contained 10.16% of lard for this purpose). After 100 days of experimental diet, pancreas were collected.

In vitro culture of acinar cells and treatments

AR42J cells from ATCC are a rat pancreatic acinar cell line. They were cultured in Advance Dulbecco's Modified Eagle's Medium F12 containing 10% FBS (Eurobio), 1% L-glutamine (Sigma-Aldrich) 1% Peniciline-streptomycin (Sigma-Aldrich). Acinar-to-ductal transdifferentiation was induced with 1 µM Dexamethasone and 10 ng/ml EGF (for 8 days). The culture medium containing diluted agents and inhibitors was changed every 48 h.

RT-qPCR analyses

Cells were harvested on ice, washed twice with cold PBS, collected, and frozen at -80°C. RNA of cell pellets was isolated according TRIzol protocol (Life Technologies). RT-qPCR reactions were carried out using RevertAid H Minus Reverse Transcriptase (Thermo Fisher) and SsoFast EvaGreen Supermix (Bio-Rad) according to the manufacturers' instructions. The list of primers is in Suppl Table 2.

Western blot analysis

Cells were harvested on ice, washed twice with cold PBS, collected, and frozen at -80°C. Dry pellets of cells were lysed in 50 mM Tris-HCl, pH 7.5, 150 mM NaCl, 1 mM EDTA, 1% Triton-X100 (Sigma-Aldrich) supplemented with protease and phosphatase inhibitors (sodium orthovanadate (Sigma-Aldrich), 1 mM DTT, 2 mM NaF (Sigma-Aldrich) and cOMPLETE Mini Protease Inhibitor Cocktail (Roche). Derivatization of carbonyl groups in protein lysates was performed according to standard

protocol (Ab178020). Protein concentration was measured using BCA Protein Assay kit (Interchim), and equal amounts of proteins were subjected to SDS-PAGE and transferred onto nitrocellulose membrane (BioTraceNT; Pall Corp). Membranes were washed in Tris Buffered Saline supplemented with 0.1% Tween-20 (TBS-T) then saturated in TBS-T with 5% non-fat dry milk, incubated overnight with primary antibodies in TBS-T with 5% BSA, washed and revealed according to Cell Signaling Technology protocol. Western blotting was conducted using standard methods with antibodies as described in the Supplementary Table 2.

Biochemical analysis

Activity PHGDH

Protein extraction was performed on cells using cold PHGDH assay buffer. Protein concentration was determined using BCA assay. Protein precipitation was performed using protein extract and saturated ammonium sulfate solution. PHGDH activity is determined using PHGDH Assay kit from Abcam ab273328, following the instructions, with PHGDH developer solution and PHGDH substrate. The luminescence is followed using CLARIOstar spectrophotometer at 37°C at 450nm.

Real-time metabolic analysis

Measurements were performed using the Seahorse Bioscience XFe24 Extracellular Flux Analyzer (Agilent). This device allows the measurement of the cellular oxygen consumption rate (OCR in pmoles/min) and of the extracellular acidification rate (ECAR in mpH/min), for mitochondrial respiration (OXPHOS) and glycolysis, respectively. Forty-eight hours before the assay, cells at exponential growth were seeded into Seahorse 24-well plates and cultured at 37°C with 5% CO_2. The number of seeded cells was optimized to ensure 70%–80% confluence the day of analysis. Twenty-four hour after seeding, cells are treated with the indicated combination of inhibitors and incubated at 37°C with 5% CO_2.

XF Cell Mito Stress Test (OXPHOS experiment)

OCR was measured using the Seahorse XF Cell Mito Stress Test Kit. Culture medium was replaced with OXPHOS assay medium (Seahorse XF base medium, 2 mM glutamine, 1 mM sodium pyruvate and 10 mM glucose, pH 7.4) and the plate was pre-incubated for 1h at 37°C in an incubator without CO_2. OCR was measured under basal conditions, and then after sequential injections of different reagents: 1 µM oligomycin (respiratory Complex V inhibitor that allows to calculate ATP production by mitochondrion), carbonyl cyanide-p-trifluoromethox- yphenyl-hydrazon (FCCP; an uncoupling agent allowing determination of the maximal respiration and the spare capacity; 1µM), and finally 0.5 µM rotenone + 0.5 µM antimycin A (Complex I and III inhibitors, respectively) to stop mitochondrial respiration enabling the calculation of the background (i.e., non-mitochondrial respiration driven by processes outside the mitochondria). Levels of OCR were normalized to 25,000 seeded cells, which we found as the most accurate way to normalize when comparing different cell types.

siRNA transfection

Cells were transfected with Lipofectamine RNAiMAX (ThermoFisher Scientific) with SMARTpool ON-TARGETplus rat siRNA (Dharmacon) targeting: Phgdh according to the manufacturer's protocols as used in(Thibault et al., 2021). ON-TARGETplus Non-targeting control siRNAs (Dharmacon) were used as controls. Forty-eight hours after transfection, the cell protein contents were extracted and analysed by western blot to determine the efficacy of siRNA transfection using anti-PHGDH antibody.

Cell processes analysis

Cell proliferation/morphological changes are estimated using the confluence followed by phase microscopy using Incucyte. Cells are incubated for seventy-two hours in 96 well plate. Two pictures by well are taken using 10x objective. Using Incucyte software the cell surface is measure on the

picture, a mean of each replicate is used to compare the different condition at the different time points.

Acinar cell isolation
Mice were anesthetized with isofluorane and sacrificed by cervical dislocation. Pancreas were quickly resected, rinsed and 100 mg of the organ were placed in 5 ml of cold HBSS (Hank's balanced salt solution) containing 0.01% (w/v) Soybean Trypsin Inhibitor (STI, Sigma-Aldrich) and 1000U of collagenase II (Thermofisher). Digestion was performed at 37°C during 20 minutes and mechanical dissociation every 5 minutes through 10 back-and-forth passages of the pancreatic tissue into sterile serological pipettes of decreasing size (25, 10 and 5 ml). Following multiple washes with HBSS supplemented with 5% FCS, 0.01% STI and 10 mM Hepes (pH 7.5), digested pancreatic tissue was pelleted by 400 rpm centrifugation, resuspended in DMEM culture medium containing 4.5 g/l glucose, 10% fetal calf serum (FCS) (Eurobio), 10% penicillin-streptomycin mixture, 0.01% STI and filtered through 100 µm-Nylon mesh.

EdU assay
Isolated acinar cells were placed in Ibidi 8 well plate coated with gelatine at 37% and 5% CO2. After 48h plating, cell are treated for 24h using the indicated inhibitor combination. To determine the inhibitor effects on cell proliferation, cells are incubated with 10µM EdU solution in the last 2 hours at 37°C with 5% CO_2. Cells are fixed using PFA for 15min and permeabilised using a solution of PBS containing 0.5% Triton-100x for 20 min. The EdU integration is revealed using the indicated solution. DAPI coloration was performed for 1min to quantify all nuclei. Edu incorporation is observed using Operetta immunofluorescence microscope. EdU positive nuclei were quantified using Harmony software.

Statistics
Experimental data provided at least three biological replicates. Data were analyzed by 2-tailed, unpaired Student's t-test or ANOVA test using a multiple statistics Graph Pad Prism software package. A difference was considered significant when p value was lower than 0.05: * $P < 0.05$, ** $P < 0.01$, *** $P < 0.001$. Non-significant (ns) if $P > 0.05$.

All authors had access to the study data and had reviewed and approved the final manuscript.

Acknowledgments
We thank all members of SigDYN, past and present, for their technical support, sample banks, common tools, scientific and protocol discussions, Arnaud Besson for IHC p27 antibody, Anexplo team work, Christèle Segura (I2MC, Inserm 1048, Toulouse, France) for part of histology sample preparation, EZOP for Inrae animal facility, Imagin (FX Fresnois) for image scanning, the CRCT core technology platform, Lorie Friedman (Genentech) for their kind gift, Pierre Cordelier for access to its microscope, Anne Couvelard for explaining the scoring method of pancreatitis and taking time to read the slides with us. JGG, MD were members of COST action EU-Pancreas BM1204. Rats from red-meat enriched diet and contraol diet were from the study funded by JPI HDHL « Meatic » https://www.healthydietforhealthylife.eu/76-hdhl-intimic-cofunded-call/393-meatic; Faecal Microbiome as determinant of the effect of diet on colorectal cancer risk: comparison of meat based versus pesco-vegetarian diets; pancreas were dissected at the same time for this study. JGG's laboratory belongs to Toucan, Laboratoire d'Excellence, ANR, an integrated research program on Signal-targeted Drug Resistance. JGG's laboratory for this topic was/is funded by Europe EU-ERG FP7 (270696 PaCa/PI3K), ARC (PJA2021060003932, PJA20171206596, PJA20141201744; salary for RB), Toucan ANR Laboratory of Excellence, MSCA-ITN/ETN PhD-PI3K (Project ID: 675392, salary for SA), Fondation de France (salary for BT), ANR-JCJC (RADIANCE-salary for BT), GSO, Ligue Nationale Contre le Cancer (salary for CC). SA disseminated their research to high school students, as part of their commitment in MSCA-ITN funding.

DB and AVV were funded by Erasmus + program. F Pierre, F Guéraud have some research projects from their academic research teams that have been co-financed by the processed meat sector. The other authors declare no conflict of interest.

Figure legends

Figure 1: **PI3K/Akt pathway and PHGDH are differentially activated/expressed in chronic pancreatitis compared to pancreatic adenocarcinoma.**

a.-c. We used raw data from various transcriptomic studies (Löhr et al., 2010; Vaquerizas et al., 2009; Rückert et al., 2008) with compatible platforms and re-analyzed them. **a.** An unbiased search of HALLMARKS differentially expressed in CP vs PDAC patients was performed; only hallmarks with p value <0.05 are shown. **b.** Statistical analysis (p values of enrichment scores) of Reactome PI3K pathway enrichment in PDAC vs normal, CP vs normal or CP vs PDAC is shown. Intensity is shown with a threshold at 0.05. **c.** Clustering of human PI3Kα gene expression signature was performed by R in normal, CP (alcoholic pancreatitis, autoimmune pancreatitis), pancreatic ductal adenocarcinoma (PDAC) and microdissected stroma from chronic pancreatitis of undocumented aetiology. Blue = low expression, Red = high expression. The unsupervised hierarchy of each sample is shown in the top part of the figure; the unsupervised hierarchy of genes is shown on the left; the list of genes is detailed on the right, with statistical differences between PDAC and CP samples. BH-corrected Q values are represented. Statistical analysis is detailed in Supplementary Table 1.

d.-h. We used the raw data of a time course evolution of gene expression previously performed in WT (black line) or KrasG12D (blue line) genetic contexts upon caerulein-induced inflammation (Kong et al., 2018) and reanalyzed gene expression in time. Times 0.5h-3h corresponds to early genes, 6h-48h middle genes, 48h-340h late genes. **d.** Scheme. **e.-g.** An unbiased pathway analysis (Reactome) was performed and, for each reactome lists presenting PI3K in their title, SES enrichment scores are represented in time. Doted rectangle points out the time points at which the differential signature is observed between the two conditions. **h.** A heat map of gene expression (PI3Kα signature) shows the differential expression of these genes in time in the two genetic contexts. *PHGDH* is high only in WT background upon Caerulein treatment (highlighted line), at a time point when FGFR1/4-PI3K signatures are significantly increased in this genetic context.

Figure 2: **Repetitive nutritive stress promotes PHGDH increased expression and is associated with PI3K activation and a decrease of proliferative markers**

a. Experimental setup describing experimental chronic pancreatitis model in mice. **b.** Representative H&E. **c.** Quantification of IHC against PHGDH (n=3 mice in each group).

d. Experimental setup describing experimental diet enriched in red meat in rats. **e.** Representative H&E. **f-g.** WB and quantification of indicated proteins (n>3 in each group). pSerAKT levels are normalized with levels of AKT; other markers with β-actin.

N≥3 biological replicates; Values are mean ± SEM. ANOVA tests: *:p<0.05; **: p<0.01; ***:p<0.001

Figure 3: **PI3Kα promotes cell proliferation in PHGDH-high acinar cells**

a. IHC against PHGDH in vehicle vs. caerulein-injected pancreas: a representative image is shown (n=3 in each group). a=acini; ADM=acinar-to-ductal metaplasia **b.** AR42J-B13 cells were treated or not (Vehicle named acinar) for 8 days with Dex + EGF (named ADM-like); representative morphology is shown. **c.** mRNA levels of indicated target genes (duct-specific genes: *CK19, CK7*; acinar-specific genes: *PTF1A, AMY2A, CTRC, MIST1*) were assessed by RT-qPCR in acinar vs ADM-like cells. (n=5 independent experiments). **d.** mRNA levels of indicated target genes (PI3Kα activation signature) were assessed by RT-qPCR in acinar vs ADM-like cells. (n=5 independent experiments). **e.** Gene ontocology PANTHER analysis of PI3Kα gene signature. Intensity False Discovery Rate is shown in scaled colors. **f.** Protein levels of indicated proteins were assessed by WB in ADM-like relative to acinar cells; quantification is normalised with β-actin levels (n=3 independent experiments). **g-h.** Protein and phospho-proteins levels of indicated target proteins were assessed by WB in acinar vs ADM-like cells; cells were treated or not with GDC-0326 (100nM) for 24h. (n=3). **i,j.** Protein levels of

indicated target proteins were assessed by WB in Vehicle cells after transfection with scramble or PHGDH smart pools of siRNAs. **k.** Protein levels of indicated target proteins were assessed by WB in acinar cells after treatment with two PHGDH pharmacological inhibitors (NCT-503, 2.5µM; CBR-5884, 30µM). Cells were treated or not with GDC-0326 (100nM) for 24h. (n=3).
l-o. Seahorse analysis indicative of glycolysis and mitochondrial activity levels was performed in 8-days Vehicle (acinar) vs Dex+EGF (ADM-like) cells. (n=4 independent experiments). Cells were treated or not with PI3Kα (GDC-0326, 100nM) or PHGDH inhibitor (CBR-5884, 30µM) for 24h.
p. CT or α^{in}E mice were injected with tamoxifen; 2.5 weeks after acini were prepared and analysed as indicated. Cre+ genotype was verified by PCR. **q.** After 2 days of culture, rate of EdU incorporation (2h pulse) was assessed by imaging with Operetta in CT+Tamox or α^{in}E+Tamox acini with or without CBR-5884, 30µM. Quantifications are shown. (n>4).
N≥3 independent experiments; Values are mean ± SEM. T-Test compared to Vehicle (2 conditions) or ANOVA tests (multiple conditions): *:p<0.05; **: p<0.01; ***:p<0.001

Figure 4: **Genetic or pharmacological inactivation of PI3Kα increases the number of proliferating acinar cells during inflammatory stress; reversely, peak treatments with PI3Kα activators promote pancreatic plasticity over parenchyma turnover.**
a. Experimental setup describing chronic pancreatitis model. **b-c.** H&E was performed on pancreas from indicated condition and genotype. Scoring of pancreatitis or metaplasic ducts in Caerulein-treated pancreas harvested at day 17 from indicated genotype. The proportion of pathological lobules / ADM was scored using 2 whole slide scans from each mouse, n=6 mice for each genotype. Values are mean ± SEM. T-Test: *=P<0.05. Representative pictures are shown. Scale bars=50µm. Black arrowheads indicate lesions.
d-g. IHC staining as indicated in WT or α^{in}C pancreas subjected to the repeated injury chronic pancreatitis protocol (Caerulein). Scale: 20µm. Representative pictures are shown. a=acini; adm=acinar-to-ductal metaplasia; s=stroma; d=normal ducts. Black and white arrowheads, stars indicate representative positive stainings for CK19 or Ki67, respectively. Positive cells or nuclei are quantified in five randomly pictured fields in each mouse. N≥4 mice. Values are mean ± SEM. T-Test: *=P<0.05.
h-i. Dosage schedule of PI3Kα-targeting drug (GDC-0326 10mg/kg daily- green arrow) in WT mice subjected to repeated pancreatitis protocol (red arrows) compared to vehicle treated mice (black arrows). n≥4 mice in each group. H&E and picrosirius coloration as indicated in vehicle- or GDC-0326-dosed and caerulein-treated WT pancreas. Representative pictures are shown. Scale bar=20µm.
j. Graphical abstract.

Suppl. Fig. 1 **PHGDH activity.** PHGDH inhibitors were added in vitro in extracts of acinar AR4-2J cells.

Suppl. Fig. 2 **Supplementary data related to in vivo experimental setups. a.** Genotyping of cre-recombined *pik3ca* allele in Cre negative or Pdx1-Cre;p110$\alpha^{lox/lox}$ (α^{in}C) pancreata. Representative results in 4 different mice are shown; the amplicon corresponds to the recombined allele (Rec) which is absent in WT pancreas. **b.** α-Amylase measurements in 10µL plasma diluted 1/20 times was performed at indicated times. α-Amylase activity in arbitrary unit is shown and represented as mean ± SEM. T-Test: **=P<0.01. **d-e.** Picrosirius red staining as indicated in WT or α^{in}C pancreas subjected to the repeated injury chronic pancreatitis protocol (Caerulein). Scale: 20µm. Representative pictures are shown. Quantification as indicated. Positive staining are quantified in five randomly pictured fields in each mouse. N≥4 mice. Values are mean ± SEM. T-Test: *=P<0.05. **f.** IHC staining as indicated in WT or α^{in}C pancreas subjected to the repeated injury chronic pancreatitis protocol (Caerulein). Scale: 20µm. Representative pictures are shown.

Supplementary Table 1 **Statistical analysis of Hallmarks gene signatures and PI3Kα-regulated gene expression in normal, CP (from alcoholic or auto-immune origin), PDAC or microdissected stroma**

of CP patients. Assembled mean values of alcoholic CP, autoimmune CP, CP stroma, normal or PDAC pancreas are shown; p-value and BH-corrected p-value are shown for PDAC vs. normal, or all vs. normal statistical tests. Lists of genes as indicated.

Supplementary Table 2 **List of tools and protocols.**

References

Al-Adsani, A., Z.D. Burke, D. Eberhard, K.L. Lawrence, C.-N. Shen, A.K. Rustgi, H. Sakaue, J.M. Farrant, and D. Tosh. 2010. Dexamethasone treatment induces the reprogramming of pancreatic acinar cells to hepatocytes and ductal cells. *PLoS ONE*. 5:e13650. doi:10.1371/journal.pone.0013650.

Albrecht, M., D. Stichel, B. Müller, R. Merkle, C. Sticht, N. Gretz, U. Klingmüller, K. Breuhahn, and F. Matthäus. 2017. TTCA: an R package for the identification of differentially expressed genes in time course microarray data. *BMC Bioinformatics*. 18:33. doi:10.1186/s12859-016-1440-8.

Arcucci, S., F. Ramos-Delgado, C. Cayron, N. Therville, M.-P. Gratacap, C. Basset, B. Thibault, and J. Guillermet-Guibert. 2021. Organismal roles for the PI3Kα and β isoforms: their specificity, redundancy or cooperation is context-dependent. *Biochemical Journal*. 478:1199–1225. doi:10.1042/BCJ20210004.

Ardito, C.M., B.M. Grüner, K.K. Takeuchi, C. Lubeseder-Martellato, N. Teichmann, P.K. Mazur, K.E. DelGiorno, E.S. Carpenter, C.J. Halbrook, J.C. Hall, D. Pal, T. Briel, A. Herner, M. Trajkovic-Arsic, B. Sipos, G.-Y. Liou, P. Storz, N.R. Murray, D.W. Threadgill, M. Sibilia, M.K. Washington, C.L. Wilson, R.M. Schmid, E.W. Raines, H.C. Crawford, and J.T. Siveke. 2012. EGF Receptor Is Required for KRAS-Induced Pancreatic Tumorigenesis. *Cancer Cell*. 22:304–317. doi:10.1016/j.ccr.2012.07.024.

Baer, R., C. Cintas, M. Dufresne, S. Cassant-Sourdy, N. Schönhuber, L. Planque, H. Lulka, B. Couderc, C. Bousquet, B. Garmy-Susini, B. Vanhaesebroeck, S. Pyronnet, D. Saur, and J. Guillermet-Guibert. 2014. Pancreatic cell plasticity and cancer initiation induced by oncogenic Kras is completely dependent on wild-type PI 3-kinase p110α. *Genes Dev*. 28:2621–2635. doi:10.1101/gad.249409.114.

Bailey, J.M., A.M. Hendley, K.J. Lafaro, M.A. Pruski, N.C. Jones, J. Alsina, M. Younes, A. Maitra, F. McAllister, C.A. Iacobuzio-Donahue, and S.D. Leach. 2016. p53 mutations cooperate with oncogenic Kras to promote adenocarcinoma from pancreatic ductal cells. *Oncogene*. 35:4282–4288. doi:10.1038/onc.2015.441.

Blasco, M.T., C. Navas, G. Martín-Serrano, O. Graña-Castro, C.G. Lechuga, L. Martín-Díaz, M. Djurec, J. Li, L. Morales-Cacho, L. Esteban-Burgos, J. Perales-Patón, E. Bousquet-Mur, E. Castellano, H.K.C. Jacob, L. Cabras, M. Musteanu, M. Drosten, S. Ortega, F. Mulero, B. Sainz, N. Dusetti, J. Iovanna, F. Sánchez-Bueno, M. Hidalgo, H. Khiabanian, R. Rabadán, F. Al-Shahrour, C. Guerra, and M. Barbacid. 2019. Complete Regression of Advanced Pancreatic Ductal Adenocarcinomas upon Combined Inhibition of EGFR and C-RAF. *Cancer Cell*. 35:573-587.e6. doi:10.1016/j.ccell.2019.03.002.

Bosch, A., Z. Li, A. Bergamaschi, H. Ellis, E. Toska, A. Prat, J.J. Tao, D.E. Spratt, N.T. Viola-Villegas, P. Castel, G. Minuesa, N. Morse, J. Rodón, Y. Ibrahim, J. Cortes, J. Perez-Garcia, P. Galvan, J. Grueso, M. Guzman, J.A. Katzenellenbogen, M. Kharas, J.S. Lewis, M. Dickler, V. Serra, N.

Rosen, S. Chandarlapaty, M. Scaltriti, and J. Baselga. 2015. PI3K inhibition results in enhanced estrogen receptor function and dependence in hormone receptor-positive breast cancer. *Sci Transl Med*. 7:283ra51. doi:10.1126/scitranslmed.aaa4442.

Bournet, B. 2014. Role of endoscopic ultrasound in the molecular diagnosis of pancreatic cancer. *WJG*. 20:10758. doi:10.3748/wjg.v20.i31.10758.

Bousquet, C., J. Guillermet-Guibert, N. Saint-Laurent, E. Archer-Lahlou, F. Lopez, M. Fanjul, A. Ferrand, D. Fourmy, C. Pichereaux, B. Monsarrat, L. Pradayrol, J.-P. Estève, and C. Susini. 2006. Direct binding of p85 to sst2 somatostatin receptor reveals a novel mechanism for inhibiting PI3K pathway. *EMBO J.* 25:3943–3954. doi:10.1038/sj.emboj.7601279.

Bouvier, A.M., N. Bossard, M. Colonna, A. Garcia-Velasco, M. Carulla, S. Manfredi, and G.E.-W. Group. 2017a. Trends in net survival from pancreatic cancer in six European Latin countries: results from the SUDCAN population-based study. *European journal of cancer prevention: the official journal of the European Cancer Prevention Organisation.* 26 Trends in cancer net survival in six European Latin Countries: the SUDCAN study:S63–S69. doi:10.1097/CEJ.0000000000000303.

Bouvier, A.M., Z. Uhry, V. Jooste, A. Drouillard, L. Remontet, G. Launoy, N. Leone, and R. French Network of Cancer. 2017b. Focus on an unusual rise in pancreatic cancer incidence in France. *International journal of epidemiology*. 46:1764–1772. doi:10.1093/ije/dyx088.

Carrière, C., A.L. Young, J.R. Gunn, D.S. Longnecker, and M. Korc. 2011. Acute pancreatitis accelerates initiation and progression to pancreatic cancer in mice expressing oncogenic Kras in the nestin cell lineage. *PLoS One*. 6:e27725. doi:10.1371/journal.pone.0027725.

Del Poggetto, E., I.-L. Ho, C. Balestrieri, E.-Y. Yen, S. Zhang, F. Citron, R. Shah, D. Corti, G.R. Diaferia, C.-Y. Li, S. Loponte, F. Carbone, Y. Hayakawa, G. Valenti, S. Jiang, L. Sapio, H. Jiang, P. Dey, S. Gao, A.K. Deem, S. Rose-John, W. Yao, H. Ying, A.D. Rhim, G. Genovese, T.P. Heffernan, A. Maitra, T.C. Wang, L. Wang, G.F. Draetta, A. Carugo, G. Natoli, and A. Viale. 2021. Epithelial memory of inflammation limits tissue damage while promoting pancreatic tumorigenesis. *Science*. 373:eabj0486. doi:10.1126/science.abj0486.

Diakopoulos, K.N., M. Lesina, S. Wörmann, L. Song, M. Aichler, L. Schild, A. Artati, W. Römisch-Margl, T. Wartmann, R. Fischer, Y. Kabiri, H. Zischka, W. Halangk, I.E. Demir, C. Pilsak, A. Walch, C.S. Mantzoros, J.M. Steiner, M. Erkan, R.M. Schmid, H. Witt, J. Adamski, and H. Algül. 2015. Impaired autophagy induces chronic atrophic pancreatitis in mice via sex- and nutrition-dependent processes. *Gastroenterology*. 148:626-638.e17. doi:10.1053/j.gastro.2014.12.003.

Friedlander, S.Y.G., G.C. Chu, E.L. Snyder, N. Girnius, G. Dibelius, D. Crowley, E. Vasile, R.A. DePinho, and T. Jacks. 2009. Context-Dependent Transformation of Adult Pancreatic Cells by Oncogenic K-Ras. *Cancer Cell*. 16:379–389. doi:10.1016/j.ccr.2009.09.027.

Goncalves, M.D., B.D. Hopkins, and L.C. Cantley. 2018. Phosphatidylinositol 3-Kinase, Growth Disorders, and Cancer. *N. Engl. J. Med.* 379:2052–2062. doi:10.1056/NEJMra1704560.

Graupera, M., J. Guillermet-Guibert, L.C. Foukas, L.-K. Phng, R.J. Cain, A. Salpekar, W. Pearce, S. Meek, J. Millan, P.R. Cutillas, A.J.H. Smith, A.J. Ridley, C. Ruhrberg, H. Gerhardt, and B. Vanhaesebroeck. 2008. Angiogenesis selectively requires the p110alpha isoform of PI3K to control endothelial cell migration. *Nature*. 453:662–666. doi:10.1038/nature06892.

Grimont, A., A.V. Pinho, M.J. Cowley, C. Augereau, A. Mawson, M. Giry-Laterrière, G. Van den Steen, N. Waddell, M. Pajic, C. Sempoux, J. Wu, S.M. Grimmond, A.V. Biankin, F.P. Lemaigre, I. Rooman, and P. Jacquemin. 2015. SOX9 regulates ERBB signalling in pancreatic cancer development. *Gut*. 64:1790–1799. doi:10.1136/gutjnl-2014-307075.

Gu, G., J.R. Brown, and D.A. Melton. 2003. Direct lineage tracing reveals the ontogeny of pancreatic cell fates during mouse embryogenesis. *Mech Dev*. 120:35–43. doi:10.1016/s0925-4773(02)00330-1.

Guerra, C., A.J. Schuhmacher, M. Canamero, P.J. Grippo, L. Verdaguer, L. Perez-Gallego, P. Dubus, E.P. Sandgren, and M. Barbacid. 2007. Chronic pancreatitis is essential for induction of pancreatic ductal adenocarcinoma by K-Ras oncogenes in adult mice. *Cancer cell.* 11:291–302. doi:10.1016/j.ccr.2007.01.012.

Guillermet-Guibert, J., K. Bjorklof, A. Salpekar, C. Gonella, F. Ramadani, A. Bilancio, S. Meek, A.J.H. Smith, K. Okkenhaug, and B. Vanhaesebroeck. 2008. The p110beta isoform of phosphoinositide 3-kinase signals downstream of G protein-coupled receptors and is functionally redundant with p110gamma. *Proc. Natl. Acad. Sci. U.S.A.* 105:8292–8297. doi:10.1073/pnas.0707761105.

Gukovsky, I., J.H. Cheng, K.J. Nam, O.T. Lee, A. Lugea, L. Fischer, J.M. Penninger, S.J. Pandol, and A.S. Gukovskaya. 2004. Phosphatidylinositide 3-kinase gamma regulates key pathologic responses to cholecystokinin in pancreatic acinar cells. *Gastroenterology*. 126:554–566.

Halbrook, C.J., H.-J. Wen, J.M. Ruggeri, K.K. Takeuchi, Y. Zhang, M.P. di Magliano, and H.C. Crawford. 2017. Mitogen-activated Protein Kinase Kinase Activity Maintains Acinar-to-Ductal Metaplasia and Is Required for Organ Regeneration in Pancreatitis. *Cell Mol Gastroenterol Hepatol*. 3:99–118. doi:10.1016/j.jcmgh.2016.09.009.

Heffron, T.P., R.A. Heald, C. Ndubaku, B. Wei, M. Augistin, S. Do, K. Edgar, C. Eigenbrot, L. Friedman, E. Gancia, P.S. Jackson, G. Jones, A. Kolesnikov, L.B. Lee, J.D. Lesnick, C. Lewis, N. McLean, M. Mörtl, J. Nonomiya, J. Pang, S. Price, W.W. Prior, L. Salphati, S. Sideris, S.T. Staben, S. Steinbacher, V. Tsui, J. Wallin, D. Sampath, and A.G. Olivero. 2016. The Rational Design of Selective Benzoxazepin Inhibitors of the α-Isoform of Phosphoinositide 3-Kinase Culminating in the Identification of (*S*)-2-((2-(1-Isopropyl-1 *H* -1,2,4-triazol-5-yl)-5,6-dihydrobenzo[*f*]imidazo[1,2- *d*][1,4]oxazepin-9-yl)oxy)propanamide (GDC-0326). *J. Med. Chem.* 59:985–1002. doi:10.1021/acs.jmedchem.5b01483.

Jeannot, P., C. Callot, R. Baer, N. Duquesnes, C. Guerra, J. Guillermet-Guibert, O. Bachs, and A. Besson. 2015. Loss of p27Kip(1) promotes metaplasia in the pancreas via the regulation of Sox9 expression. *Oncotarget*. 6:35880–92. doi:10.18632/oncotarget.5770.

Kawaguchi, Y., J.-C. Lin, Y. Kawashima, A. Maruno, H. Ito, M. Ogawa, and T. Mine. 2015. Relationship between Pain and Plasma Amino Acid Levels in Chronic Pancreatitis. *JOP. Journal of the Pancreas*. Vol 16:53-57 Pages. doi:10.6092/1590-8577/2897.

Kirkegård, J., D. Cronin-Fenton, U. Heide-Jørgensen, and F.V. Mortensen. 2018. Acute Pancreatitis and Pancreatic Cancer Risk: A Nationwide Matched-Cohort Study in Denmark. *Gastroenterology*. 154:1729–1736. doi:10.1053/j.gastro.2018.02.011.

Kleeff, J., E. Costello, R. Jackson, C. Halloran, W. Greenhalf, P. Ghaneh, R.F. Lamb, M.M. Lerch, J. Mayerle, D. Palmer, T. Cox, C.L. Rawcliffe, O. Strobel, M.W. Büchler, and J.P. Neoptolemos.

2016a. The impact of diabetes mellitus on survival following resection and adjuvant chemotherapy for pancreatic cancer. *Br J Cancer*. 115:887–894. doi:10.1038/bjc.2016.277.

Kleeff, J., M. Korc, M. Apte, C. La Vecchia, C.D. Johnson, A.V. Biankin, R.E. Neale, M. Tempero, D.A. Tuveson, R.H. Hruban, and J.P. Neoptolemos. 2016b. Pancreatic cancer. *Nat Rev Dis Primers*. 2:16022. doi:10.1038/nrdp.2016.22.

Kleeff, J., D.C. Whitcomb, T. Shimosegawa, I. Esposito, M.M. Lerch, T. Gress, J. Mayerle, A.M. Drewes, V. Rebours, F. Akisik, J.E.D. Muñoz, and J.P. Neoptolemos. 2017. Chronic pancreatitis. *Nat Rev Dis Primers*. 3:17060. doi:10.1038/nrdp.2017.60.

Klein, A.P. 2021. Pancreatic cancer epidemiology: understanding the role of lifestyle and inherited risk factors. *Nat Rev Gastroenterol Hepatol*. 18:493–502. doi:10.1038/s41575-021-00457-x.

Kong, B., P. Bruns, N.A. Behler, L. Chang, A.M. Schlitter, J. Cao, A. Gewies, J. Ruland, S. Fritzsche, N. Valkovskaya, Z. Jian, I. Regel, S. Raulefs, M. Irmler, J. Beckers, H. Friess, M. Erkan, N.S. Mueller, S. Roth, T. Hackert, I. Esposito, F.J. Theis, J. Kleeff, and C.W. Michalski. 2018. Dynamic landscape of pancreatic carcinogenesis reveals early molecular networks of malignancy. *Gut*. 67:146–156. doi:10.1136/gutjnl-2015-310913.

Kopp, J.L., G. von Figura, E. Mayes, F.-F. Liu, C.L. Dubois, J.P. Morris, F.C. Pan, H. Akiyama, C.V.E. Wright, K. Jensen, M. Hebrok, and M. Sander. 2012. Identification of Sox9-dependent acinar-to-ductal reprogramming as the principal mechanism for initiation of pancreatic ductal adenocarcinoma. *Cancer Cell*. 22:737–750. doi:10.1016/j.ccr.2012.10.025.

Li, A.M., and J. Ye. 2020. The PHGDH enigma: Do cancer cells only need serine or also a redox modulator? *Cancer Lett*. 476:97–105. doi:10.1016/j.canlet.2020.01.036.

Locasale, J.W., A.R. Grassian, T. Melman, C.A. Lyssiotis, K.R. Mattaini, A.J. Bass, G. Heffron, C.M. Metallo, T. Muranen, H. Sharfi, A.T. Sasaki, D. Anastasiou, E. Mullarky, N.I. Vokes, M. Sasaki, R. Beroukhim, G. Stephanopoulos, A.H. Ligon, M. Meyerson, A.L. Richardson, L. Chin, G. Wagner, J.M. Asara, J.S. Brugge, L.C. Cantley, and M.G. Vander Heiden. 2011. Phosphoglycerate dehydrogenase diverts glycolytic flux and contributes to oncogenesis. *Nat Genet*. 43:869–874. doi:10.1038/ng.890.

Löhr, J.-M., R. Faissner, D. Koczan, P. Bewerunge, C. Bassi, B. Brors, R. Eils, L. Frulloni, A. Funk, W. Halangk, R. Jesenofsky, L. Kaderali, J. Kleeff, B. Krüger, M.M. Lerch, R. Lösel, M. Magnani, M. Neumaier, S. Nittka, M. Sahin-Tóth, J. Sänger, S. Serafini, M. Schnölzer, H.-J. Thierse, S. Wandschneider, G. Zamboni, and G. Klöppel. 2010. Autoantibodies against the exocrine pancreas in autoimmune pancreatitis: gene and protein expression profiling and immunoassays identify pancreatic enzymes as a major target of the inflammatory process. *Am J Gastroenterol*. 105:2060–2071. doi:10.1038/ajg.2010.141.

Lupia, E., A. Goffi, P. De Giuli, O. Azzolino, O. Bosco, E. Patrucco, M.C. Vivaldo, M. Ricca, M.P. Wymann, E. Hirsch, G. Montrucchio, and G. Emanuelli. 2004. Ablation of phosphoinositide 3-kinase-gamma reduces the severity of acute pancreatitis. *Am. J. Pathol.* 165:2003–2011.

Ma, C., K. Zheng, K. Jiang, Q. Zhao, N. Sha, W. Wang, M. Yan, T. Chen, Y. Zhao, and Y. Jiang. 2021. The alternative activity of nuclear PHGDH contributes to tumour growth under nutrient stress. *Nat Metab*. 3:1357–1371. doi:10.1038/s42255-021-00456-x.

Meyers, N., C. Gérard, F.P. Lemaigre, and P. Jacquemin. 2020. Differential impact of the ERBB receptors EGFR and ERBB2 on the initiation of precursor lesions of pancreatic ductal adenocarcinoma. *Sci Rep*. 10:5241. doi:10.1038/s41598-020-62106-8.

Molina-Montes, E., P. Gomez-Rubio, M. Márquez, M. Rava, M. Löhr, C.W. Michalski, X. Molero, A. Farré, J. Perea, W. Greenhalf, L. Ilzarbe, M. O'Rorke, A. Tardón, T. Gress, V.M. Barberà, T. Crnogorac-Jurcevic, E. Domínguez-Muñoz, L. Muñoz-Bellvís, J. Balsells, E. Costello, J. Huang, M. Iglesias, J. Kleeff, B. Kong, J. Mora, L. Murray, D. O'Driscoll, I. Poves, A. Scarpa, W. Ye, M. Hidalgo, L. Sharp, A. Carrato, F.X. Real, N. Malats, and the PanGenEU Study Investigators. 2018. Risk of pancreatic cancer associated with family history of cancer and other medical conditions by accounting for smoking among relatives. *International Journal of Epidemiology*. 47:473–483. doi:10.1093/ije/dyx269.

Navas, C., I. Hernández-Porras, A.J. Schuhmacher, M. Sibilia, C. Guerra, and M. Barbacid. 2012. EGF receptor signaling is essential for k-ras oncogene-driven pancreatic ductal adenocarcinoma. *Cancer Cell*. 22:318–330. doi:10.1016/j.ccr.2012.08.001.

Ngo, B., E. Kim, V. Osorio-Vasquez, S. Doll, S. Bustraan, R.J. Liang, A. Luengo, S.M. Davidson, A. Ali, G.B. Ferraro, G.M. Fischer, R. Eskandari, D.S. Kang, J. Ni, A. Plasger, V.K. Rajasekhar, E.R. Kastenhuber, S. Bacha, R.K. Sriram, B.D. Stein, S.F. Bakhoum, M. Snuderl, P. Cotzia, J.H. Healey, N. Mainolfi, V. Suri, A. Friedman, M. Manfredi, D.M. Sabatini, D.R. Jones, M. Yu, J.J. Zhao, R.K. Jain, K.R. Keshari, M.A. Davies, M.G. Vander Heiden, E. Hernando, M. Mann, L.C. Cantley, and M.E. Pacold. 2020. Limited Environmental Serine and Glycine Confer Brain Metastasis Sensitivity to PHGDH Inhibition. *Cancer Discov*. 10:1352–1373. doi:10.1158/2159-8290.CD-19-1228.

Nöthlings, U., L.R. Wilkens, S.P. Murphy, J.H. Hankin, B.E. Henderson, and L.N. Kolonel. 2005. Meat and Fat Intake as Risk Factors for Pancreatic Cancer: The Multiethnic Cohort Study. *JNCI: Journal of the National Cancer Institute*. 97:1458–1465. doi:10.1093/jnci/dji292.

Pacold, M.E., K.R. Brimacombe, S.H. Chan, J.M. Rohde, C.A. Lewis, L.J.Y.M. Swier, R. Possemato, W.W. Chen, L.B. Sullivan, B.P. Fiske, S. Cho, E. Freinkman, K. Birsoy, M. Abu-Remaileh, Y.D. Shaul, C.M. Liu, M. Zhou, M.J. Koh, H. Chung, S.M. Davidson, A. Luengo, A.Q. Wang, X. Xu, A. Yasgar, L. Liu, G. Rai, K.D. Westover, M.G. Vander Heiden, M. Shen, N.S. Gray, M.B. Boxer, and D.M. Sabatini. 2016. A PHGDH inhibitor reveals coordination of serine synthesis and one-carbon unit fate. *Nat Chem Biol*. 12:452–458. doi:10.1038/nchembio.2070.

Pandol, S.J., A.K. Saluja, C.W. Imrie, and P.A. Banks. 2007. Acute Pancreatitis: Bench to the Bedside. *Gastroenterology*. 133:1056.e1-1056.e25. doi:10.1053/j.gastro.2007.08.026.

Petrick, J.L., N. Castro-Webb, H. Gerlovin, T.N. Bethea, S. Li, E.A. Ruiz-Narváez, L. Rosenberg, and J.R. Palmer. 2020. A Prospective Analysis of Intake of Red and Processed Meat in Relation to Pancreatic Cancer among African American Women. *Cancer Epidemiology, Biomarkers & Prevention*. 29:1775–1783. doi:10.1158/1055-9965.EPI-20-0048.

Pons-Tostivint, E., B. Thibault, and J. Guillermet-Guibert. 2017. Targeting PI3K Signaling in Combination Cancer Therapy. *Trends Cancer*. 3:454–469. doi:10.1016/j.trecan.2017.04.002.

Possemato, R., K.M. Marks, Y.D. Shaul, M.E. Pacold, D. Kim, K. Birsoy, S. Sethumadhavan, H.-K. Woo, H.G. Jang, A.K. Jha, W.W. Chen, F.G. Barrett, N. Stransky, Z.-Y. Tsun, G.S. Cowley, J. Barretina, N.Y. Kalaany, P.P. Hsu, K. Ottina, A.M. Chan, B. Yuan, L.A. Garraway, D.E. Root, M. Mino-Kenudson, E.F. Brachtel, E.M. Driggers, and D.M. Sabatini. 2011. Functional genomics reveal

that the serine synthesis pathway is essential in breast cancer. *Nature*. 476:346–350. doi:10.1038/nature10350.

Puri, S., A.E. Folias, and M. Hebrok. 2015. Plasticity and dedifferentiation within the pancreas: development, homeostasis, and disease. *Cell Stem Cell*. 16:18–31. doi:10.1016/j.stem.2014.11.001.

Raju, J. 2008. Azoxymethane-induced rat aberrant crypt foci: relevance in studying chemoprevention of colon cancer. *World J Gastroenterol*. 14:6632–6635. doi:10.3748/wjg.14.6632.

Reid, M.A., A.E. Allen, S. Liu, M.V. Liberti, P. Liu, X. Liu, Z. Dai, X. Gao, Q. Wang, Y. Liu, L. Lai, and J.W. Locasale. 2018. Serine synthesis through PHGDH coordinates nucleotide levels by maintaining central carbon metabolism. *Nat Commun*. 9:5442. doi:10.1038/s41467-018-07868-6.

Riscal, R., E. Schrepfer, G. Arena, M.Y. Cissé, F. Bellvert, M. Heuillet, F. Rambow, E. Bonneil, F. Sabourdy, C. Vincent, I. Ait-Arsa, T. Levade, P. Thibaut, J.-C. Marine, J.-C. Portais, J.-E. Sarry, L. Le Cam, and L.K. Linares. 2016. Chromatin-Bound MDM2 Regulates Serine Metabolism and Redox Homeostasis Independently of p53. *Molecular Cell*. 62:890–902. doi:10.1016/j.molcel.2016.04.033.

Rossi, M., P. Altea-Manzano, M. Demicco, G. Doglioni, L. Bornes, M. Fukano, A. Vandekeere, A.M. Cuadros, J. Fernández-García, C. Riera-Domingo, C. Jauset, M. Planque, H.F. Alkan, D. Nittner, D. Zuo, L.A. Broadfield, S. Parik, A.A. Pane, F. Rizzollo, G. Rinaldi, T. Zhang, S.T. Teoh, A.B. Aurora, P. Karras, I. Vermeire, D. Broekaert, J.V. Elsen, M.M.L. Knott, M.F. Orth, S. Demeyer, G. Eelen, L.E. Dobrolecki, A. Bassez, T.V. Brussel, K. Sotlar, M.T. Lewis, H. Bartsch, M. Wuhrer, P. van Veelen, P. Carmeliet, J. Cools, S.J. Morrison, J.-C. Marine, D. Lambrechts, M. Mazzone, G.J. Hannon, S.Y. Lunt, T.G.P. Grünewald, M. Park, J. van Rheenen, and S.-M. Fendt. 2022. PHGDH heterogeneity potentiates cancer cell dissemination and metastasis. *Nature*. 605:747–753. doi:10.1038/s41586-022-04758-2.

Rückert, F., M. Hennig, C.D. Petraki, D. Wehrum, M. Distler, A. Denz, M. Schröder, G. Dawelbait, H. Kalthoff, H.-D. Saeger, E.P. Diamandis, C. Pilarsky, and R. Grützmann. 2008. Co-expression of KLK6 and KLK10 as prognostic factors for survival in pancreatic ductal adenocarcinoma. *Br J Cancer*. 99:1484–1492. doi:10.1038/sj.bjc.6604717.

Shen, B., Y. Li, C.-S. Sheng, L. Liu, T. Hou, N. Xia, S. Sun, Y. Miao, Y. Pang, K. Gu, X. Lu, C. Wen, Y. Cheng, Y. Yang, D. Wang, Y. Zhu, M. Cheng, K. Harris, Z.T. Bloomgarden, J. Tian, J. Chalmers, and Y. Shi. 2023. Association between age at diabetes onset or diabetes duration and subsequent risk of pancreatic cancer: results from a longitudinal cohort and mendelian randomization study. *The Lancet Regional Health - Western Pacific*. 30:100596. doi:10.1016/j.lanwpc.2022.100596.

Siegel, R.L., K.D. Miller, and A. Jemal. 2017. Cancer Statistics, 2017. *CA Cancer J Clin*. 67:7–30. doi:10.3322/caac.21387.

Siegel, R.L., K.D. Miller, N.S. Wagle, and A. Jemal. 2023. Cancer statistics, 2023. *CA A Cancer J Clinicians*. 73:17–48. doi:10.3322/caac.21763.

Stanger, B.Z., and M. Hebrok. 2013. Control of cell identity in pancreas development and regeneration. *Gastroenterology*. 144:1170–1179. doi:10.1053/j.gastro.2013.01.074.

Storz, P., and H.C. Crawford. 2020. Carcinogenesis of Pancreatic Ductal Adenocarcinoma. *Gastroenterology*. 158:2072–2081. doi:10.1053/j.gastro.2020.02.059.

Strobel, O., Y. Dor, J. Alsina, A. Stirman, G. Lauwers, A. Trainor, C.F.-D. Castillo, A.L. Warshaw, and S.P. Thayer. 2007. In vivo lineage tracing defines the role of acinar-to-ductal transdifferentiation in inflammatory ductal metaplasia. *Gastroenterology*. 133:1999–2009. doi:10.1053/j.gastro.2007.09.009.

Thibault, B., F. Ramos-Delgado, E. Pons-Tostivint, N. Therville, C. Cintas, S. Arcucci, S. Cassant-Sourdy, G. Reyes-Castellanos, M. Tosolini, A.V. Villard, C. Cayron, R. Baer, J. Bertrand-Michel, D. Pagan, D. Ferreira Da Mota, H. Yan, C. Falcomatà, F. Muscari, B. Bournet, J.-P. Delord, E. Aksoy, A. Carrier, P. Cordelier, D. Saur, C. Basset, and J. Guillermet-Guibert. 2021. Pancreatic cancer intrinsic PI3Kα activity accelerates metastasis and rewires macrophage component. *EMBO Mol Med*. 13:e13502. doi:10.15252/emmm.202013502.

Tosolini, M., C. Algans, F. Pont, B. Ycart, and J.-J. Fournié. 2016. Large-scale microarray profiling reveals four stages of immune escape in non-Hodgkin lymphomas. *Oncoimmunology*. 5:e1188246. doi:10.1080/2162402X.2016.1188246.

Vanhaesebroeck, B., J. Guillermet-Guibert, M. Graupera, and B. Bilanges. 2010. The emerging mechanisms of isoform-specific PI3K signalling. *Nat. Rev. Mol. Cell Biol.* 11:329–341. doi:10.1038/nrm2882.

Vaquerizas, J.M., S.K. Kummerfeld, S.A. Teichmann, and N.M. Luscombe. 2009. A census of human transcription factors: function, expression and evolution. *Nat Rev Genet*. 10:252–263. doi:10.1038/nrg2538.

Wollny, D., S. Zhao, I. Everlien, X. Lun, J. Brunken, D. Brüne, F. Ziebell, I. Tabansky, W. Weichert, A. Marciniak-Czochra, and A. Martin-Villalba. 2016. Single-Cell Analysis Uncovers Clonal Acinar Cell Heterogeneity in the Adult Pancreas. *Dev. Cell*. 39:289–301. doi:10.1016/j.devcel.2016.10.002.

Wu, C.-Y.C., E.S. Carpenter, K.K. Takeuchi, C.J. Halbrook, L.V. Peverley, H. Bien, J.C. Hall, K.E. DelGiorno, D. Pal, Y. Song, C. Shi, R.Z. Lin, and H.C. Crawford. 2014. PI3K regulation of RAC1 is required for KRAS-induced pancreatic tumorigenesis in mice. *Gastroenterology*. 147:1405-1416.e7. doi:10.1053/j.gastro.2014.08.032.

Zhang, Y., P. Kwok-Shing Ng, M. Kucherlapati, F. Chen, Y. Liu, Y.H. Tsang, G. de Velasco, K.J. Jeong, R. Akbani, A. Hadjipanayis, A. Pantazi, C.A. Bristow, E. Lee, H.S. Mahadeshwar, J. Tang, J. Zhang, L. Yang, S. Seth, S. Lee, X. Ren, X. Song, H. Sun, J. Seidman, L.J. Luquette, R. Xi, L. Chin, A. Protopopov, T.F. Westbrook, C.S. Shelley, T.K. Choueiri, M. Ittmann, C. Van Waes, J.N. Weinstein, H. Liang, E.P. Henske, A.K. Godwin, P.J. Park, R. Kucherlapati, K.L. Scott, G.B. Mills, D.J. Kwiatkowski, and C.J. Creighton. 2017. A Pan-Cancer Proteogenomic Atlas of PI3K/AKT/mTOR Pathway Alterations. *Cancer Cell*. 31:820-832.e3. doi:10.1016/j.ccell.2017.04.013.

Zhao, X., J. Fu, J. Du, and W. Xu. 2020. The Role of D-3-Phosphoglycerate Dehydrogenase in Cancer. *Int. J. Biol. Sci.* 16:1495–1506. doi:10.7150/ijbs.41051.

Zhou, Q., and D.A. Melton. 2018. Pancreas regeneration. *Nature*. 557:351–358. doi:10.1038/s41586-018-0088-0.

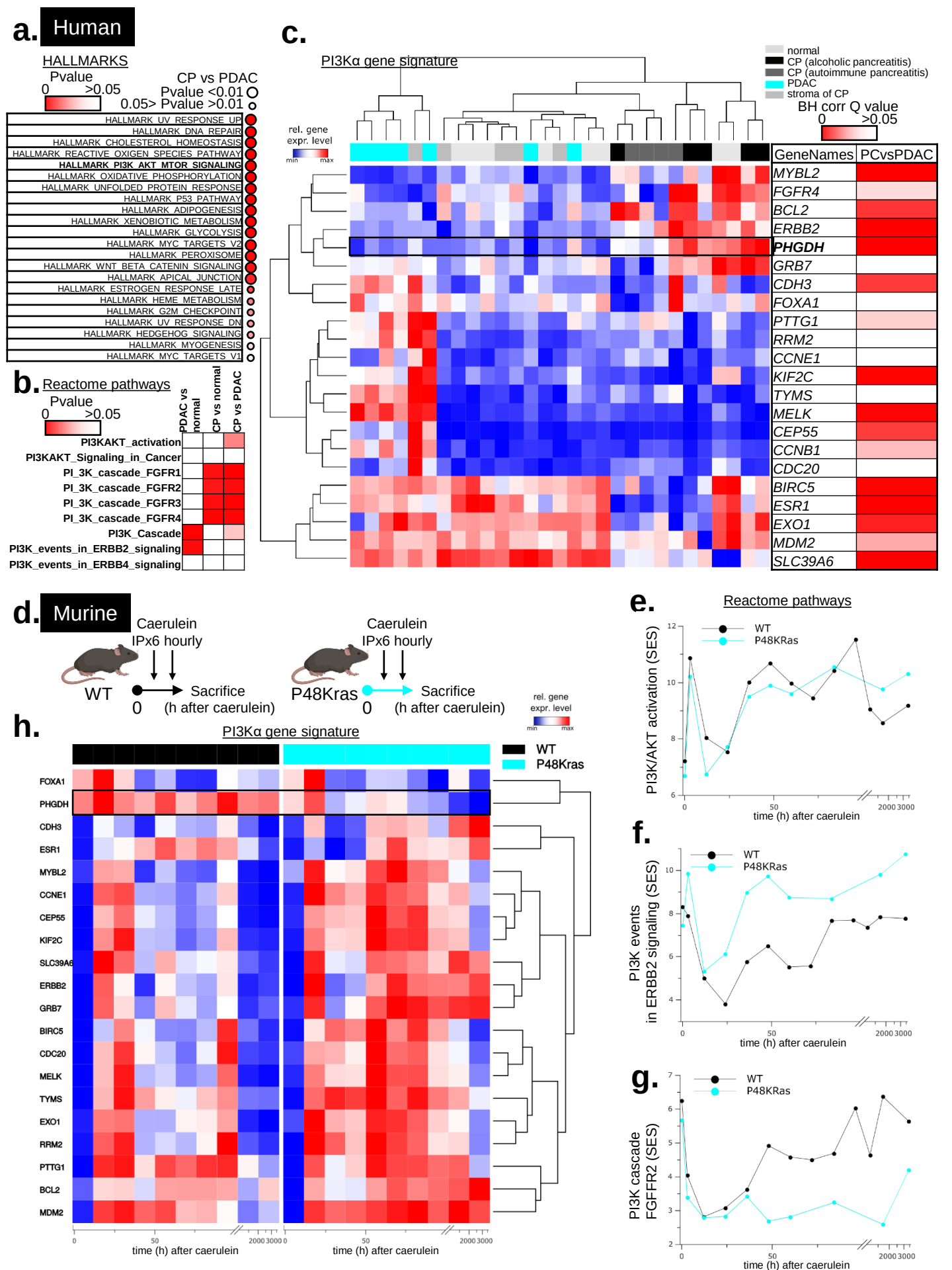
a. Human
HALLMARKS
Pvalue
0 >0.05
CP vs PDAC
Pvalue <0.01
0.05> Pvalue >0.01
HALLMARK_UV_RESPONSE_UP
HALLMARK_DNA_REPAIR
HALLMARK_CHOLESTEROL_HOMEOSTASIS
HALLMARK_REACTIVE_OXIGEN_SPECIES_PATHWAY
HALLMARK_PI3K_AKT_MTOR_SIGNALING
HALLMARK_OXIDATIVE_PHOSPHORYLATION
HALLMARK_UNFOLDED_PROTEIN_RESPONSE
HALLMARK_P53_PATHWAY
HALLMARK_ADIPOGENESIS
HALLMARK_XENOBIOTIC_METABOLISM
HALLMARK_GLYCOLYSIS
HALLMARK_MYC_TARGETS_V2
HALLMARK_PEROXISOME
HALLMARK_WNT_BETA_CATENIN_SIGNALING
HALLMARK_APICAL_JUNCTION
HALLMARK_ESTROGEN_RESPONSE_LATE
HALLMARK_HEME_METABOLISM
HALLMARK_G2M_CHECKPOINT
HALLMARK_UV_RESPONSE_DN
HALLMARK_HEDGEHOG_SIGNALING
HALLMARK_MYOGENESIS
HALLMARK_MYC_TARGETS_V1
b. Reactome pathways
Pvalue
0 >0.05
PDAC vs normal
CP vs normal
CP vs PDAC
PI3KAKT_activation
PI3KAKT_Signaling_in_Cancer
PI_3K_cascade_FGFR1
PI_3K_cascade_FGFR2
PI_3K_cascade_FGFR3
PI_3K_cascade_FGFR4
PI3K_Cascade
PI3K_events_in_ERBB2_signaling
PI3K_events_in_ERBB4_signaling
c.
PI3Kα gene signature
normal
CP (alcoholic pancreatitis)
CP (autoimmune pancreatitis)
PDAC
stroma of CP
BH corr Q value
0 >0.05
rel. gene expr. level
min max
GeneNames
PCvsPDAC
MYBL2
FGFR4
BCL2
ERBB2
PHGDH
GRB7
CDH3
FOXA1
PTTG1
RRM2
CCNE1
KIF2C
TYMS
MELK
CEP55
CCNB1
CDC20
BIRC5
ESR1
EXO1
MDM2
SLC39A6
d. Murine
Caerulein
IPx6 hourly
WT
0
Sacrifice
(h after caerulein)
Caerulein
IPx6 hourly
P48Kras
0
Sacrifice
(h after caerulein)
rel. gene expr. level
min max
h.
PI3Kα gene signature
WT
P48Kras
FOXA1
PHGDH
CDH3
ESR1
MYBL2
CCNE1
CEP55
KIF2C
SLC39A6
ERBB2
GRB7
BIRC5
CDC20
MELK
TYMS
EXO1
RRM2
PTTG1
BCL2
MDM2
0
50
2000 3000
time (h) after caerulein
e.
Reactome pathways
WT
P48KRas
PI3K/AKT activation (SES)
time (h) after caerulein
f.
WT
P48KRas
PI3K events in ERBB2 signaling (SES)
time (h) after caerulein
g.
WT
P48KRas
PI3K cascade FGFFR2 (SES)
time (h) after caerulein

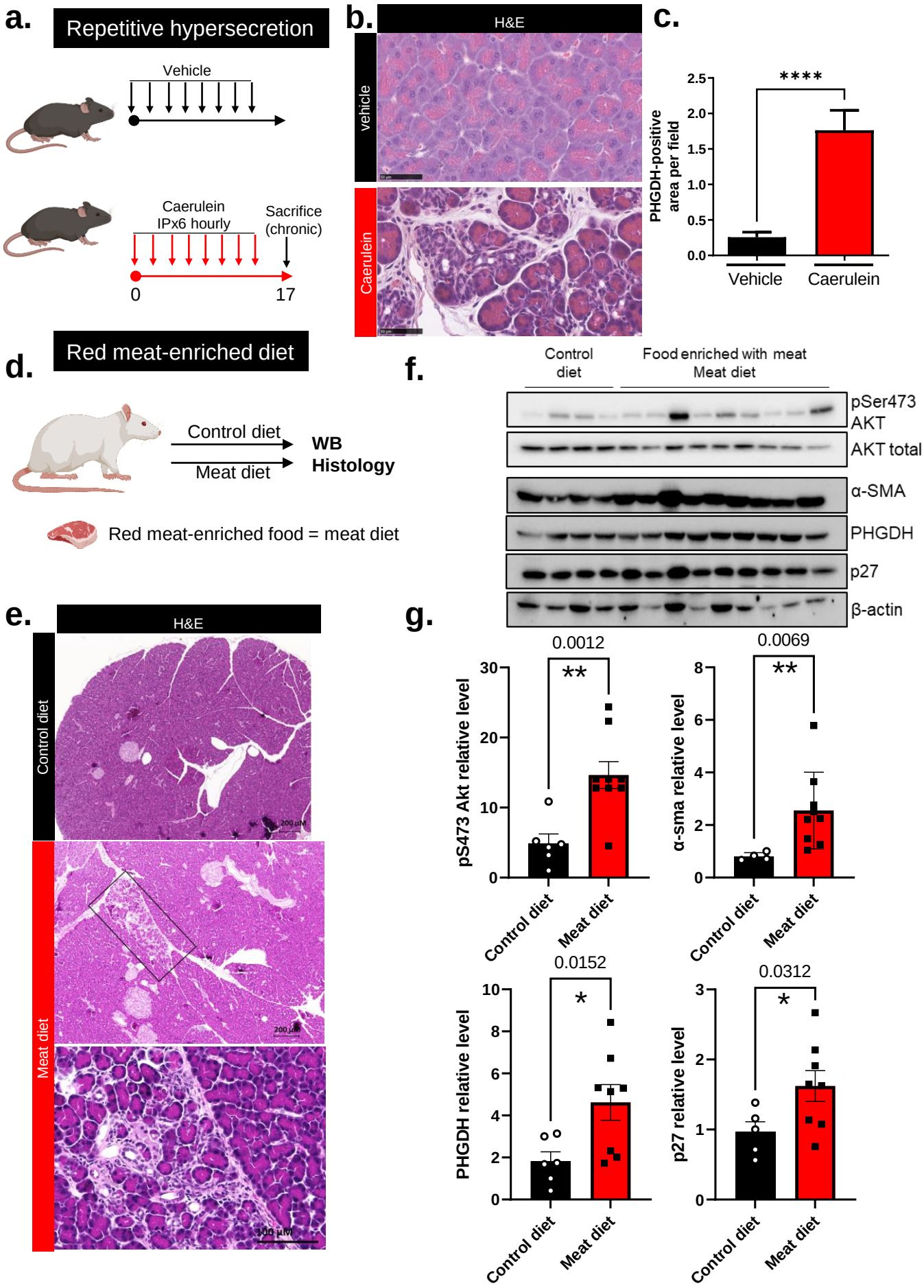
a.
Repetitive hypersecretion
Vehicle
Caerulein
IPx6 hourly
Sacrifice
(chronic)
0
17
b.
H&E
vehicle
Caerulein
c.
PHGDH-positive area per field
****
Vehicle
Caerulein
d.
Red meat-enriched diet
Control diet
Meat diet
WB
Histology
Red meat-enriched food = meat diet
f.
Control diet
Food enriched with meat
Meat diet
pSer473 AKT
AKT total
α-SMA
PHGDH
p27
β-actin
e.
H&E
Control diet
Meat diet
200 µM
100 µM
g.
0.0012
**
pS473 Akt relative level
0.0069
**
α-sma relative level
0.0152
*
PHGDH relative level
0.0312
*
p27 relative level
Control diet
Meat diet

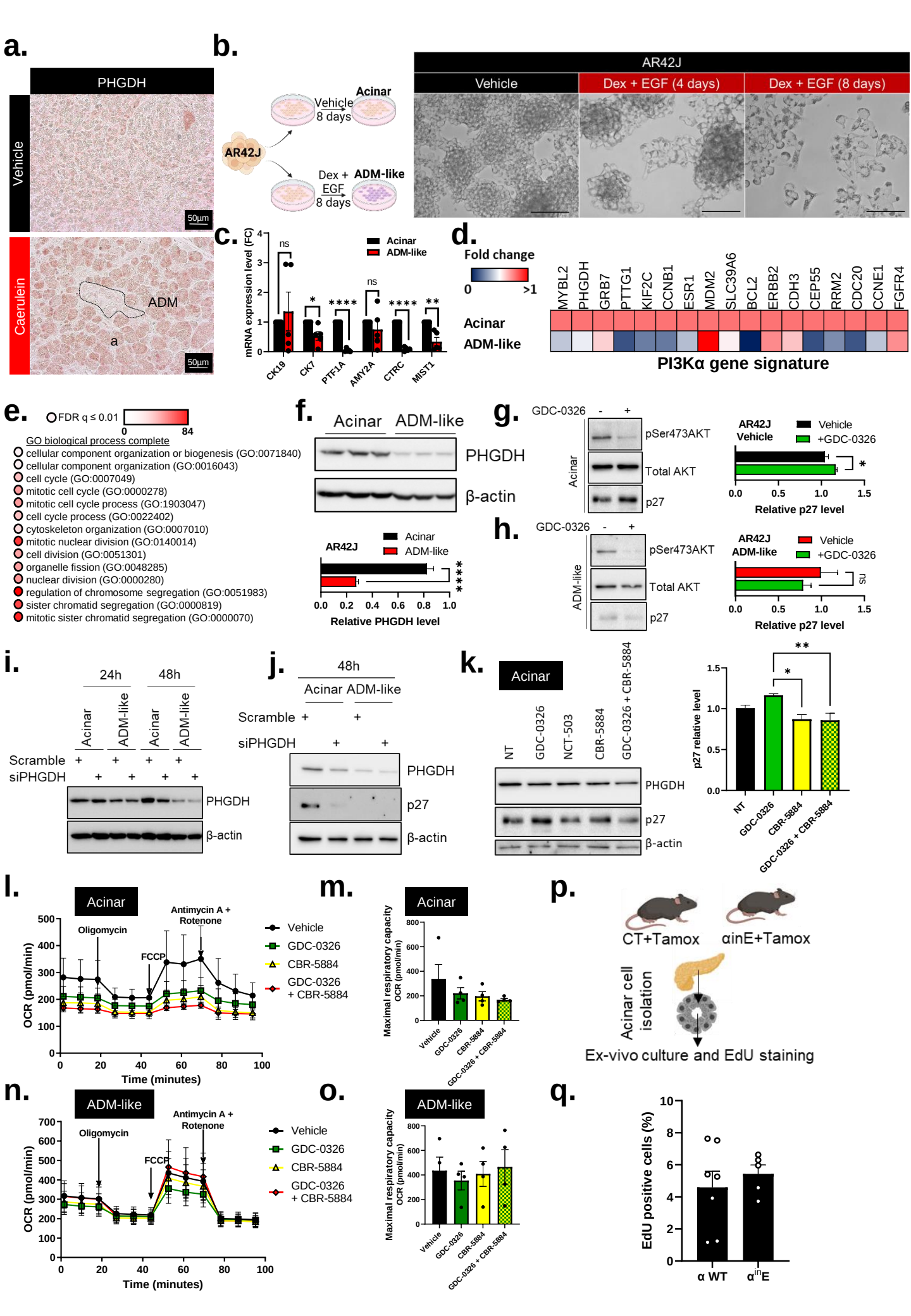
a.
PHGDH
Vehicle
Caerulein
ADM
a
50µm
b.
AR42J
Vehicle
8 days
Acinar
Dex + EGF
8 days
ADM-like
AR42J
Vehicle
Dex + EGF (4 days)
Dex + EGF (8 days)
c.
mRNA expression level (FC)
Acinar
ADM-like
ns
CK19
CK7
PTF1A
AMY2A
CTRC
MIST1
d.
Fold change
0
>1
Acinar
ADM-like
MYBL2
PHGDH
GRB7
PTTG1
KIF2C
CCNB1
ESR1
MDM2
SLC39A6
BCL2
ERBB2
CDH3
CEP55
RRM2
CDC20
CCNE1
FGFR4
PI3Kα gene signature
e.
FDR q ≤ 0.01
0
84
GO biological process complete
cellular component organization or biogenesis (GO:0071840)
cellular component organization (GO:0016043)
cell cycle (GO:0007049)
mitotic cell cycle (GO:0000278)
mitotic cell cycle process (GO:1903047)
cell cycle process (GO:0022402)
cytoskeleton organization (GO:0007010)
mitotic nuclear division (GO:0140014)
cell division (GO:0051301)
organelle fission (GO:0048285)
nuclear division (GO:0000280)
regulation of chromosome segregation (GO:0051983)
sister chromatid segregation (GO:0000819)
mitotic sister chromatid segregation (GO:0000070)
f.
Acinar
ADM-like
PHGDH
β-actin
AR42J
Acinar
ADM-like
Relative PHGDH level
g.
GDC-0326
Acinar
pSer473AKT
Total AKT
p27
AR42J
Vehicle
Vehicle
+GDC-0326
Relative p27 level
h.
GDC-0326
ADM-like
pSer473AKT
Total AKT
p27
AR42J
ADM-like
Vehicle
+GDC-0326
ns
Relative p27 level
i.
24h
48h
Acinar
ADM-like
Acinar
ADM-like
Scramble
siPHGDH
PHGDH
β-actin
j.
48h
Acinar
ADM-like
Scramble
siPHGDH
PHGDH
p27
β-actin
k.
Acinar
NT
GDC-0326
NCT-503
CBR-5884
GDC-0326 + CBR-5884
PHGDH
p27
β-actin
p27 relative level
l.
Acinar
Oligomycin
FCCP
Antimycin A + Rotenone
Vehicle
GDC-0326
CBR-5884
GDC-0326 + CBR-5884
OCR (pmol/min)
Time (minutes)
m.
Acinar
Maximal respiratory capacity OCR (pmol/min)
Vehicle
GDC-0326
CBR-5884
GDC-0326 + CBR-5884
p.
CT+Tamox
αinE+Tamox
Acinar cell isolation
Ex-vivo culture and EdU staining
n.
ADM-like
Oligomycin
FCCP
Antimycin A + Rotenone
Vehicle
GDC-0326
CBR-5884
GDC-0326 + CBR-5884
OCR (pmol/min)
Time (minutes)
o.
ADM-like
Maximal respiratory capacity OCR (pmol/min)
Vehicle
GDC-0326
CBR-5884
GDC-0326 + CBR-5884
q.
EdU positive cells (%)
α WT
αinE

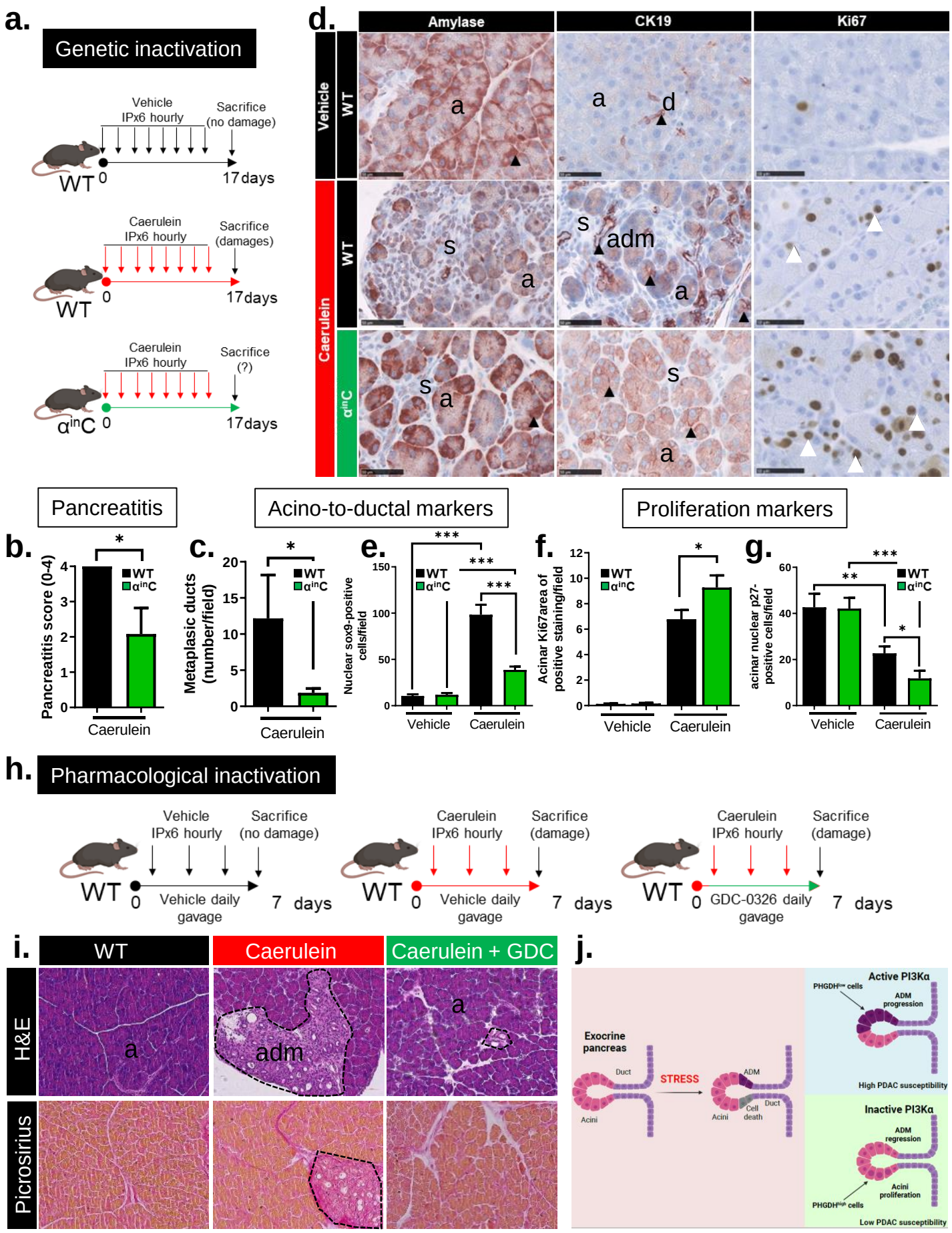
a.
Genetic inactivation
Vehicle IPx6 hourly
Sacrifice (no damage)
WT 0
17 days
Caerulein IPx6 hourly
Sacrifice (damages)
WT 0
17 days
Caerulein IPx6 hourly
Sacrifice (?)
αinC 0
17 days
d.
Amylase
CK19
Ki67
Vehicle
WT
Caerulein
WT
αinC
a
d
s
adm
Pancreatitis
Acino-to-ductal markers
Proliferation markers
b.
Pancreatitis score (0-4)
WT
αinC
Caerulein
c.
Metaplasic ducts (number/field)
e.
Nuclear sox9-positive cells/field
Vehicle
Caerulein
f.
Acinar Ki67area of positive staining/field
g.
acinar nuclear p27-positive cells/field
h.
Pharmacological inactivation
Vehicle IPx6 hourly
Sacrifice (no damage)
WT 0
Vehicle daily gavage
7 days
Caerulein IPx6 hourly
Sacrifice (damage)
WT 0
Vehicle daily gavage
7 days
Caerulein IPx6 hourly
Sacrifice (damage)
WT 0
GDC-0326 daily gavage
7 days
i.
WT
Caerulein
Caerulein + GDC
H&E
Picrosirius
a
adm
j.
Exocrine pancreas
Duct
Acini
STRESS
ADM
Cell death
Active PI3Kα
PHGDHlow cells
ADM progression
High PDAC susceptibility
Inactive PI3Kα
ADM regression
Acini proliferation
PHGDHhigh cells
Low PDAC susceptibility